SRNL-STI-2011-00025

Key Words:
Blending, Mixing,
Sludge Disturbance

Retention:
Permanent

SDI CFD MODELING ANALYSIS

Si Y. Lee
Brian W. Armstrong*
* Summer Intern

APRIL 2011

Savannah River National Laboratory
Savannah River Nuclear Solutions
Aiken, SC 29808

Prepared for the U.S. Department of Energy Under
Contract Number DE-AC09-08SR22470

DISCLAIMER

Printed in the United States of America

Prepared for
U.S. Department of Energy

SRNL-STI-2011-00025

Key Words:
Blending, Mixing,
Sludge Disturbance

Retention:
Permanent

SDI CFD MODELING ANALYSIS

Si Y. Lee
Brian W. Armstrong*
* Summer Intern

APRIL 2011

Savannah River National Laboratory
Savannah River Nuclear Solutions
Savannah River Site
Aiken, SC 29808

Prepared for the U.S. Department of Energy Under
Contract Number DE-AC09-08SR22470

TABLE OF CONTENTS

LIST OF FIGURES iv

LIST OF TABLES vi

NOMENCLATURE vii

1.0 EXECUTIVE SUMMARY 1

2.0 INTRODUCTION 3

3.0 LITERATURE REVIEW ON JET MIXING STUDIES 15
3.1 General Review 15
3.2 Basic Characteristics of Turbulent Jet Mixing / Blending 20
3.3 Review Summary 21

4.0 MODELING APPROACH AND ANALYSIS 23

5.0 RESULTS AND DISCUSSIONS 28
5.1 Benchmarking Results 33
5.2 Performance Modeling Results 47

6.0 CONCLUSIONS AND SUMMARY 66

7.0 REFERENCES 67

LIST OF FIGURES

Figure 1. Geometrical configurations [W706692] and three-dimensional modeling domain containing one blending pump and one transfer pump in the analysis of the phase-I Tank 50 performance model 6
Figure 2: Cooling coil arrangement for Tank 50 [W708852]. 7
Figure 3. Geometrical side and front views for the V-shaped EDL blending pump 9
Figure 4. Geometrical configurations for the CW blending pump used in the phase-II final performance analysis 10
Figure 5. Typical velocity profiles in the direction perpendicular to the free surface from the previous modeling results of large-scale tank mixing simulations [Lee et al, 2008]. 17
Figure 6. Computational domains of the tank models with and without cooling coils for the CFD analysis 26
Figure 7. Three-dimensional view of computational volume meshes for the tank model with no cooling coils 27
Figure 8. Three-dimensional view of computational volume meshes and representative two-dimensional meshes near the pump and cooling coils for the tank model with cooling coils 27
Figure 9. Typical flow patterns on the vertical and horizontal discharge planes of the T-shaped jet pump (Case 1) 30
Figure 10. Typical steady-state flow patterns on the vertical and horizontal discharge planes of the V-shaped jet pump (Case 11a) 31
Figure 11. Transient tracer concentrations at the pump discharge plane for Case 1 showing that number in color map indicates the non-dimensionalized value with respect to equilibrium concentration. 32
Figure 12. Comparison of steady state flow evolutions of the blending jet with the literature data along the principal discharge line inside the EDL scale tank with no coils 35
Figure 13. Positions for local velocity measurements on the tank fluid domain 35
Figure 14. Velocity flow patterns and local velocity measurement locations at 2 in elevation for the Case 1 modeling conditions 35
Figure 15. Benchmarking results of CFD predictions against the EDL and TNX test results for local velocities inside the EDL-scale tank with and without cooling coils (EDL cases: Case 1, Case 2 (2g.2.1 and 2g.2.1.a), Case 11a, 11b, and case 12a) .. 43
Figure 16. Comparison of flow velocity distributions at the plane 1 inch above the tank floor between two typical jet flow rates of 10 and 6 gpm for the EDL tank with no cooling coils 44
Figure 17. Comparison of flow velocity distributions at the plane 1 inch above the tank floor for the EDL tank without and with cooling coils for 9.95 gpm, $U_o d_o$ = 0.81 ft^2/sec under the same color map 45
Figure 18. Benchmarking results of EDL tank with no coils against the EDL test results for the water-acid blending time 46
Figure 19. Benchmarking results of EDL tank with coils against the EDL test results for the water-acid blending time 46
Figure 20. Velocity distributions at top surface of the sludge layer (Case 10). 50
Figure 21. Velocity distributions at top surface of the sludge layer (Case 11a) 50
Figure 22. Velocity distributions at top surface of the sludge layer (Case 11b). 51
Figure 23. Velocity distributions at top surface of the sludge layer (Case 12b) 51

Figure 24. Velocity distributions at top surface of the sludge layer (Case 13) 52
Figure 25. Velocity distributions at top surface of the sludge layer (Case 14) 52
Figure 26. Velocity distributions at top surface of the sludge layer (Case 15). 53
Figure 27. Velocity flow patterns at top surface of the sludge layer (Case 15). 53
Figure 29. Velocity distributions at top surface of the sludge layer (Case 16a). 55
Figure 30. Velocity distributions at top surface of the sludge layer (Case 16b). 56
Figure 31. Velocity distributions at top surface of the sludge layer for the transfer pump operations in EDL scale tank. 57
Figure 32. Velocity distributions at top surface of the sludge layer (Case 17a). 58
Figure 33. Velocity distributions at top surface of the sludge layer (Case 17b). 59
Figure 34. Velocity distributions at top surface of the sludge layer (Case 17c). 60
Figure 35. Comparison of transient blending concentrations for the T-shape pump inside the EDL tank with and without cooling coils (Nozzle speed = 46.5 ft/sec, $U_o d_o$ = 0.81 ft^2/sec) 61
Figure 36. Impact of cooling coils on the blending time for the water-acid blending time 62
Figure 37. Comparison of flow velocity distributions for the final CW pump inside the full-scale tank with and without cooling coils 65

LIST OF TABLES

Table 1. Pump design parameters for quad volute pump used for jet mixing operations at SRS....8
Table 2. Modeling cases for the analysis....11
Table 3. Transfer pump models for different transfer pump configurations and elevations under EDL pilot-scale and full-scale operations....14
Table 4. Velocity decay constant and spread rate for free turbulent jets....18
Table 5. Models and correlations for mixing time....22
Table 6. Data conditions of turbulent jets used in Fig. 12....34
Table 7. Quantitative comparison of the modeling predictions to the test results for the local positions near the tank bottom (Measurement positions of local velocities for U_od_o = 0.81 ft^2/sec.....37
Table 8. Quantitative comparison of the modeling predictions to the test results for the local positions near the tank bottom (U_od_o = 0.83 ft^2/sec, Case 2).....38
Table 9. Quantitative comparison of the modeling predictions to the test results for the local positions near the tank bottom (U_od_o = 0.81 ft^2/sec, Case2.....39
Table 10. Quantitative comparison of the modeling predictions to the test results for the local positions near the tank bottom (U_od_o = 0.58 ft^2/sec).....40
Table 11. Quantitative comparison of the modeling predictions to the test results for the local positions near the tank bottom (U_od_o = 0.58 ft^2/sec).....41
Table 12. Quantitative comparison of the modeling predictions to the test results for the local positions near the tank bottom (U_od_o = 0.70 ft^2/sec).....42
Table 13. Max. local velocity at the top sludge layer for different transfer pump configurations and elevations under full-scale operations....58
Table 14. Quantitative comparison of blending times for the EDL scale-down and full-scale tanks with T-shape pumps....61
Table 15. Quantitative comparison of blending times for two different tank scales with T-shape and V-shape pumps....62
Table 16. CFD results for the cases considered for the modeling analysis....63

NOMENCLATURE

A	Area
C	Concentration or constant for equation
C_{eq}	Equilibrium concentration
C_o	Constant used in Eq. (1)
C_μ	Constant in Eq. (3)
D	Tank diameter
D_v	Molecular diffusion coefficient
d_o	Jet nozzle diameter
E	Kinetic energy
F	Correlation constant used in Table 5.
f_{jet}	Jet mixing time factor used in Table 5
g	Gravitational acceleration
h_l	Liquid heght
k	Turbulent kinetic energy per unit mass
L	Jet length or maximum integral length scale
m_o	Mass flow rate at jet inlet
m_1	Entrained mass flow rate
p	Pressure
Δp	Pressure drop
Q	Volumetric flow rate
Q_j	Jet volumetric flow rate
R	Tank or pipe radius
R_s	Jet spreading rate
r	Local radial distance of turbulent jet region
t	Time
Sc_t	Turbulent Schmidt number (= Ratio of momentum to mass diffusion)
t_m	Mixing time
U_o	Velocity at jet nozzle exit
U	Local velocity along the jet discharge direction
u_x	Local velocity along the x-axis
u_y	Local velocity along the y-axis
u_z	Local velocity along the z-axis
x	Local distance along the x-axis
ε	Turbulent energy dissipation rate per unit mass
ε_v	Turbulent energy dissipation rate per unit volume
ρ	Fluid density
λ	Turbulent length scale
λ_B	Batchelor length scale
λ_d	Kolmogorov length scale
λ_{dif}	Diffusion length
μ_t	Turbulent dynamic viscosity (= $\rho\nu_t$)
ν	Kinematic viscosity
ν_t	Turbulent eddy diffusion coefficient
φ_v	Non-dimensional velocity distribution
Re	Reynolds number
Re_{jet}	Reynolds number based on jet operating conditions

CFD	Computational Fluid Dynamics
DOE	United States Department of Energy
EDL	Engineering Development Laboratory
FLUENT	CFD software code
QVP	Quad Volute Pump
SBP	Submersible Blender Pump
SDI	Salt Disposition Integration
SMP	Submersible Mixer Pump
SRNL	Savannah River National Laboratory
SRS	Savannah River Site
SWPF	Salt Waste Processing Facility
TTQAP	Technical Task Quality Assurance Plan
wt	weight

1.0 EXECUTIVE SUMMARY

The Savannah River Remediation (SRR) Organization requested that Savannah River National Laboratory (SRNL) develop a Computational Fluid Dynamics (CFD) method to mix and blend the miscible contents of the blend tanks to ensure the contents are properly blended before they are transferred from the blend tank; such as, Tank 50H, to the Salt Waste Processing Facility (SWPF) feed tank. The work described here consists of two modeling areas. They are the mixing modeling analysis during miscible liquid blending operation, and the flow pattern analysis during transfer operation of the blended liquid.

The transient CFD governing equations consisting of three momentum equations, one mass balance, two turbulence transport equations for kinetic energy and dissipation rate, and one species transport were solved by an iterative technique until the species concentrations of tank fluid were in equilibrium. The steady-state flow solutions for the entire tank fluid were used for flow pattern analysis, for velocity scaling analysis, and the initial conditions for transient blending calculations. A series of the modeling calculations were performed to estimate the blending times for various jet flow conditions, and to investigate the impact of the cooling coils on the blending time of the tank contents. The modeling results were benchmarked against the pilot scale test results. All of the flow and mixing models were performed with the nozzles installed at the mid-elevation, and parallel to the tank wall.

From the CFD modeling calculations, the main results are summarized as follows:

- The benchmark analyses for the CFD flow velocity and blending models demonstrate their consistency with Engineering Development Laboratory (EDL) and literature test results in terms of local velocity measurements and experimental observations. Thus, an application of the established criterion to SRS full scale tank will provide a better, physically-based estimate of the required mixing time, and elevation of transfer pump for minimum sludge disturbance.
- An empirical equation for a tank with no cooling coils agrees reasonably with the current modeling results for the dual jet.
- From the sensitivity study of the cooling coils, it was found that the tank mixing time for the coiled tank was about two times longer than that of the tank fluid with no coils under the $1/10^{th}$ scale, while the coiled tank required only 50% longer than the one without coils under the full scale Tank 50H. In addition, the time difference is reduced when the pumping $U_o d_o$ value is increased for a given tank.
- The blending time for T-shape dual jet pump is about 20% longer than that of 15^o upward V-shape pump under the $1/10^{th}$ pilot-scale tank, while the time difference between the two pumps is about 12% for the full-scale Tank 50H. These results are consistent with the literature information.
- A transfer pump with a solid-plate suction screen operating at 130 gpm can be located 9.5 inches above settled sludge for 2 in screen height in a 85 ft waste tank without disturbing any sludge. Detailed results are summarized in Table 13.

Final pump performance calculations were made by using the established CW pump design, and operating conditions to satisfy the two requirements of minimum sludge disturbance, and adequate blending of tank contents. The final calculation results show

that the blending times for the coiled and uncoiled tanks coupled with the CW pump design are 159 and 83 minutes, respectively. All the results are provided in Table 16.

2.0 INTRODUCTION

The Savannah River Remediation (SRR) Organization requested that Savannah River National Laboratory (SRNL) evaluate methods to mix and blend the contents of the blend tanks to ensure the contents are properly blended before they are transferred from the blend tank; such as, Tank 50H, to the Salt Waste Processing Facility (SWPF) feed tank. The tank contents consist of three forms: dissolved salt solution, other waste salt solutions, and sludge containing settled solids. This work focuses on minimizing disturbance of the sludge layer settled on the tank floor, while ensuring that the solutions are blended adequately above the sludge layer.

The work consists of two principal objectives to investigate two different pumps. One objective is to identify a suitable pumping arrangement that will adequately blend/mix two miscible liquids to obtain a uniform composition in the tank with a minimum level of sludge solid particulate in suspension. The other is to estimate the elevation in the tank at which the transfer pump inlet should be located where the solid concentration of the entrained fluid remains below the acceptance criterion (0.09 wt% or 1200 mg/liter) during transfer operation to the SWPF.

Computational Fluid Dynamics (CFD) approach is taken by using the three-dimensional full scale configuration of SRS Type-IIIA tank, Tank 50H, as shown in Fig. 1. As shown in the figure, major solid obstructions including the tank wall, the pump housing, the transfer pump column, and the 82-in central support column will be included in the mixing performance model. Typical slurry pump configurations are shown in Fig. 1. At full scale model, flow obstructions due to the presence of the cooling coils will be evaluated for the entire domain of the full scale tank. Detailed layout of the cooling coils inside Tank 50H as modeled for the analysis is shown in Fig. 2. Basic flow pattern behaviors used in the performance model will be benchmarked against the EDL test results with and without cooling coils. The EDL tests were performed using a 1/10.85 scale tank.

Tank 50H is a Waste Tank that will be used to prepare batches of salt feed for SWPF. The salt feed must be a homogeneous solution satisfying the acceptance criterion of the solids entrainment during transfer operation. The work scope described here consists of two modeling areas. They are the modeling analysis during miscible liquid blending operation, and the flow pattern analysis during transfer operation of the blended liquid. The modeling calculations for the blending time are performed by using the 95% homogeneity criterion for the entire liquid domain of the tank. The liquid mixing analysis includes four major cases, all of which deal with different pump configurations using a combination of pump types and tank wall boundaries, the resulting flow pattern from those configurations, and the impact of the flow pattern on particle entrainment from the sludge layer.

The four primary cases considered for the mixing analysis are:

Case-A: A 1/10.85 scale model with no cooling coils to benchmark the model against the EDL test results.

Case-B: A 1/10.85 scale model with cooling coils to benchmark the model against the EDL test results.

Case-C: Tank 50H full scale models with and without cooling coils to estimate the impact of flow obstructions on flow patterns due to the presence of cooling coils. These results will be compared with those of the EDL scale models.

Case-D: The 1/10.85 scale and full-scale models done in Case-A, -B, and -C to benchmark the modeling results for local velocities near the top sludge layer against all the test results done in the recent EDL experiments and the previous work. The results will be used in the validation of the critical velocity criterion to prevent the scouring of the solids from the sludge layer.

Conditions similar to one Quad Volute Pump (QVP) mixing pump will be used for the baseline performance analysis (Table 1). The baseline model uses one QVP in the flow domain of Tank 50H as provided in TTQAP (SRNL-RP-2010-00081). The baseline modeling conditions focus on the initial scoping calculations of blending times for a pump with horizontal dual jet nozzles; such as, the QVP, before considering the disturbance of the sludge layer. The blending pump is required to mix the tank contents, and increasing the blender pump flow rate provided better blending, while decreasing the flow minimized sludge disturbance. The two requirements for a blending pump should be optimized, and a determination of whether, or not, a range of flow rates could be established for adequate blending without sludge disturbance is a primary goal of the work. To that end, final calculations are based on a range of modeling conditions for different nozzle shape and flowrates. All the modeling conditions considered here are summarized in Table 2.

The transfer pump models are developed to estimate the elevation in the tank to keep the solid concentration of the entrained fluid below the acceptance criterion during transfer operation to the SWPF. The modeling conditions for different transfer pump configurations and elevations for EDL pilot-scale and full-scale operations are listed in Table 3.

The work described in this report establishes the pump design for blending the miscible liquids without any disturbance of the settled sludge materials. The benchmark analyses demonstrate their consistency with EDL and literature test results, and an application of the established criterion provides SRS full scale tank to provide a better, physically-based estimate of the required mixing time. A single-phase Computational Fluid Dynamics (CFD) approach is taken for the analysis of jet flow patterns with an emphasis on the velocity decay and the turbulent flow evolution for the far-field region from the pump. Literature results for a turbulent jet flow are reviewed here, since the decay of the axial jet velocity and the evolution of the jet flow patterns are important phenomena affecting sludge suspension and blending operations. The literature information indicates that the velocity at any point in the region of established flow is directly proportional to the product, $U_o d_o$. This product term for a blending pump is also referred to as pumping flow in the text.

The current work focuses on the estimate of mechanical blending time of two miscible liquids related to the turbulent dispersion stirred by the jet entrainment. In this case, maximum pumping flow of the blending pump will be determined by the acceptance criterion when the sludge layer settled at the tank floor is not disturbed during the jet blending process in full tank liquid level. The criterion will be established by the EDL (1/10.85 scale) tests and TNX full scale results.

One of the main objectives in waste processing is to provide the Salt Waste Processing Facility (SWPF) a uniform fluid composition below a specified sludge weight percentage (typically <0.09 wt%) during transfers. In preparation of the fluid blending for miscible fluids to SWPF, several important questions have been raised with regard to fluid blending of the miscible liquids in the tank:

- How much jet pumping flow is required to prepare a homogeneous fluid with a uniform fluid composition for SWPF to ensure that the blending jet does not disturb the sludge layer settled on the tank floor?
- How long will it take to mix and blend the miscible fluids for uniform composition in a specified Tank 50H waste tank?
- What are positions of blending and transfer pumps to answer the questions concerning uniform blending of miscible fluids and prevention of sludge disturbance stated above?

All modeling calculations for these blending operations are performed by a three-dimensional CFD approach. The CFD modeling results are benchmarked against the EDL test results to validate the model. Ultimately, the calculation results will not only link to the 1/10th scale testing at EDL, but it will help validate the anticipated performance of the pump vendor's design, referred to as final Curtiss Wright (CW) design in the text. Final performance calculations will be performed by using the established pump design and the operating conditions to satisfy those two requirements of minimum sludge disturbance and adequate blending of tank contents. Figure 4 show the final CW design pump with 15^{o} upward dual jets. From CW-EMD design document, the inlet screen assembly is a 18.0 inch diameter by 6.0 high cylindrical frame wrapped with a 3/8 inch mesh screen which prevents large solids from entering the submersible blender pump (SBP) hydraulics. The screen material is wire mesh of 0.120 inch diameter wire with a 0.380 inch opening between wires, and an open area of 57.6%. The total inlet screen area composed of the 18.0 inch diameter by 6.0 inch high cylinder is approximately 329 in^2. Considering the open area of the wire mesh and the blockage of the integrated radial support spokes, the total open flow area is on the order of 188 in^2

As discussed earlier, the work focuses on both aspects of tank mixing: to establish mixing criteria associated with the waste processing at SRS and to quantify the mixing time required to blend miscible fluids with the submersible jet pump. Prior to discussing the modeling approach, the literature results for a turbulent jet mixing are reviewed briefly, since the decay of the axial jet velocity and the evolution of the jet flow patterns are important phenomena affecting mixing operations.

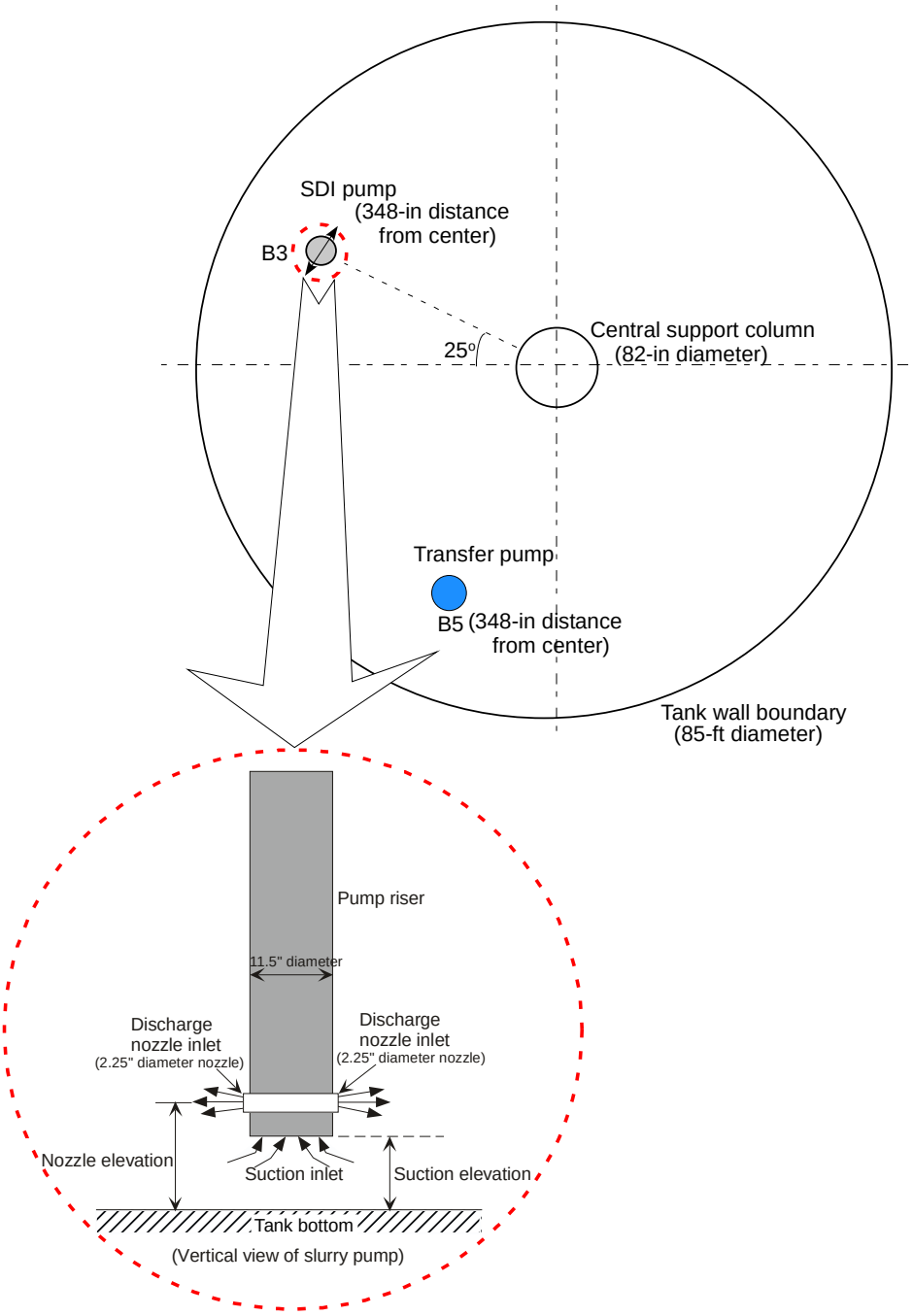

Figure 1. Geometrical configurations [W706692] and three-dimensional modeling domain containing one blending pump and one transfer pump in the analysis of the phase-I Tank 50 performance model

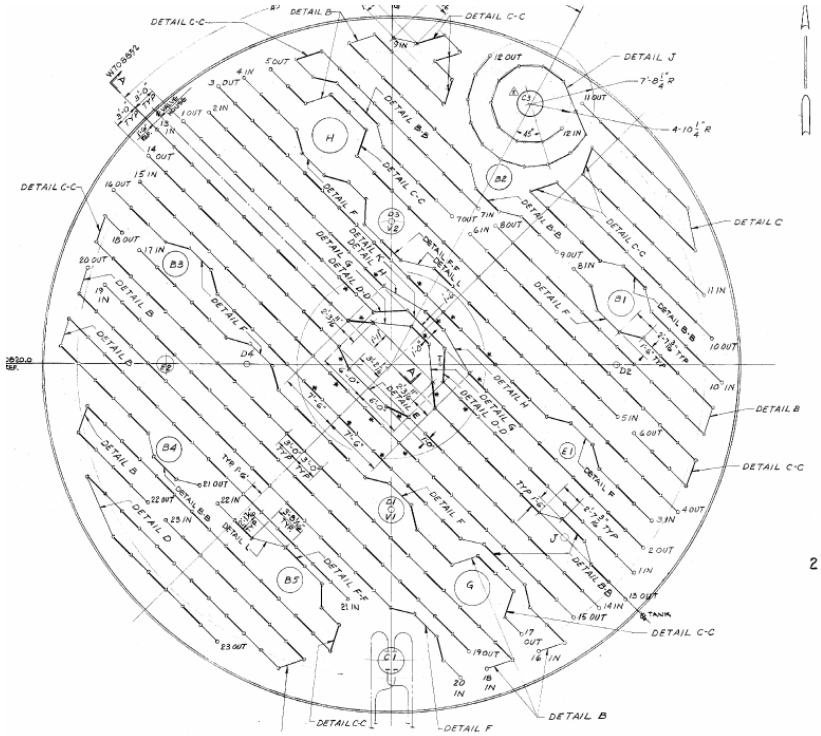

Plan View

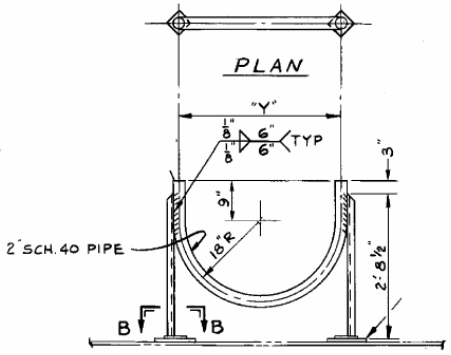

Lower coil section

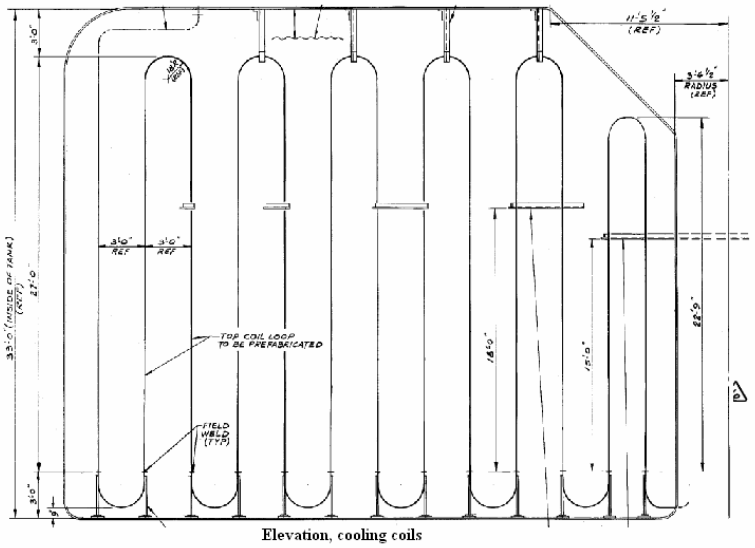

Elevation, cooling coils

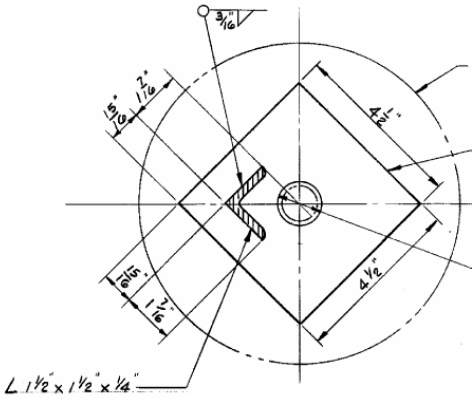

Coil, lower support, mounting plate

Figure 2: Cooling coil arrangement for Tank 50 [W708852].

Table 1. Pump design parameters for quad volute pump used for jet mixing operations at SRS

Pumps		**Quad volute pump (QVP)**	
Power, hp		300	
Number of nozzles		2	
Flow rate per nozzle, gpm		1163 (2 nozzles)	
Number of pumps		1	
Nozzle diameter, inches		Full-scale	2.25”
		EDL Scale (Reduced by ~10.85)	0.209”
Pump rotation (for the present analysis)		No (Indexed pump)	
Tank fluid	Water**	Density: 1.00 gm/ml	Viscosity: 1.00 cp
	Nitrite	1.26 gm/ml	2.35 cp
	Nitrate	1.32 gm/ml	2.26 cp
Pump nozzle elevation above tank bottom, inches		16” for EDL scale, 174” for full scale	
Velocity at nozzle exit, ft/sec (m/sec)		46.93 (14.30)	
$U_o d_o$*, $m^2 sec^{-1}$ ($ft^2 sec^{-1}$)		0.81 (8.8)**	

Note: *Final value of $U_o d_o$ determined by SRNL and SRR

**The baseline value was based on the initial scoping conditions before consideration of the velocity criterion to prevent the sludge layer disturbance.

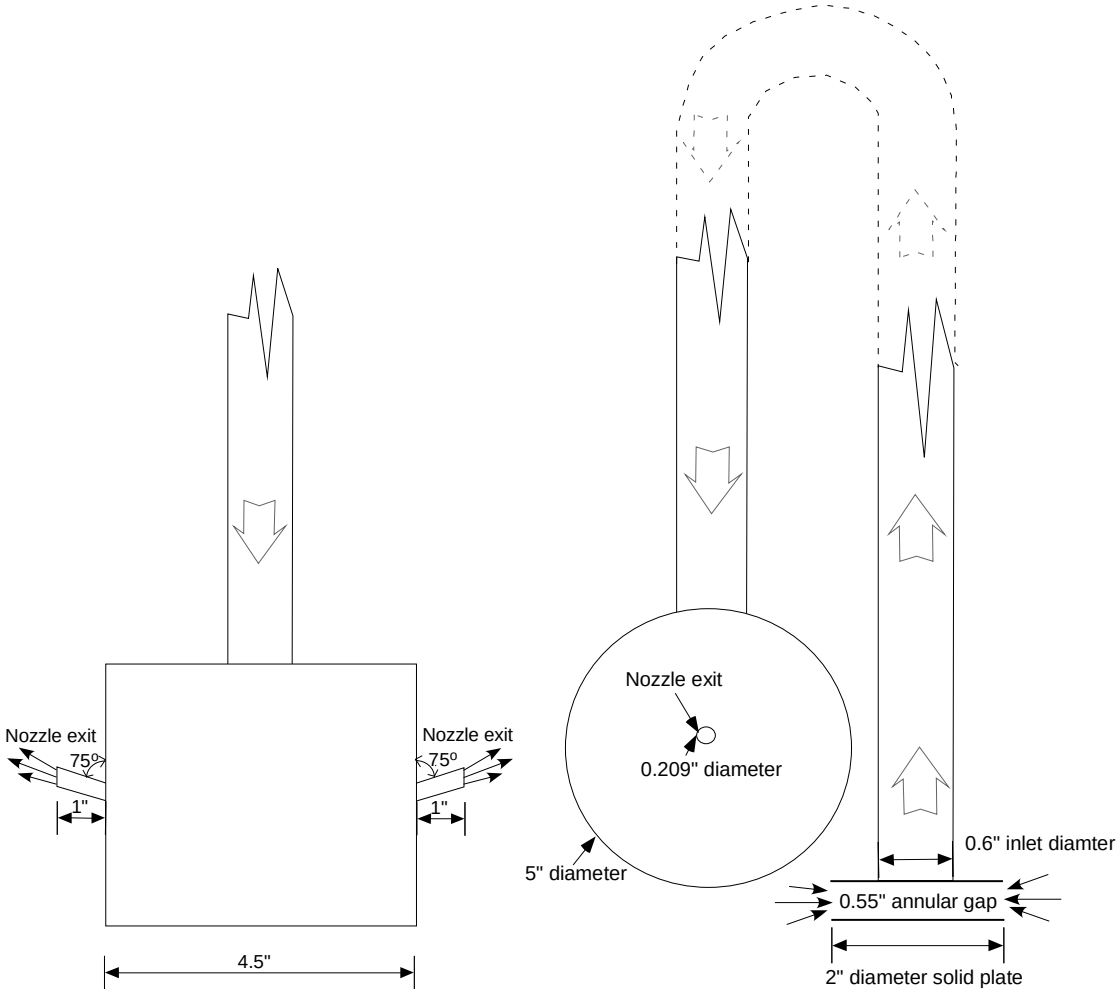

Figure 3. Geometrical side and front views for the V-shaped EDL blending pump

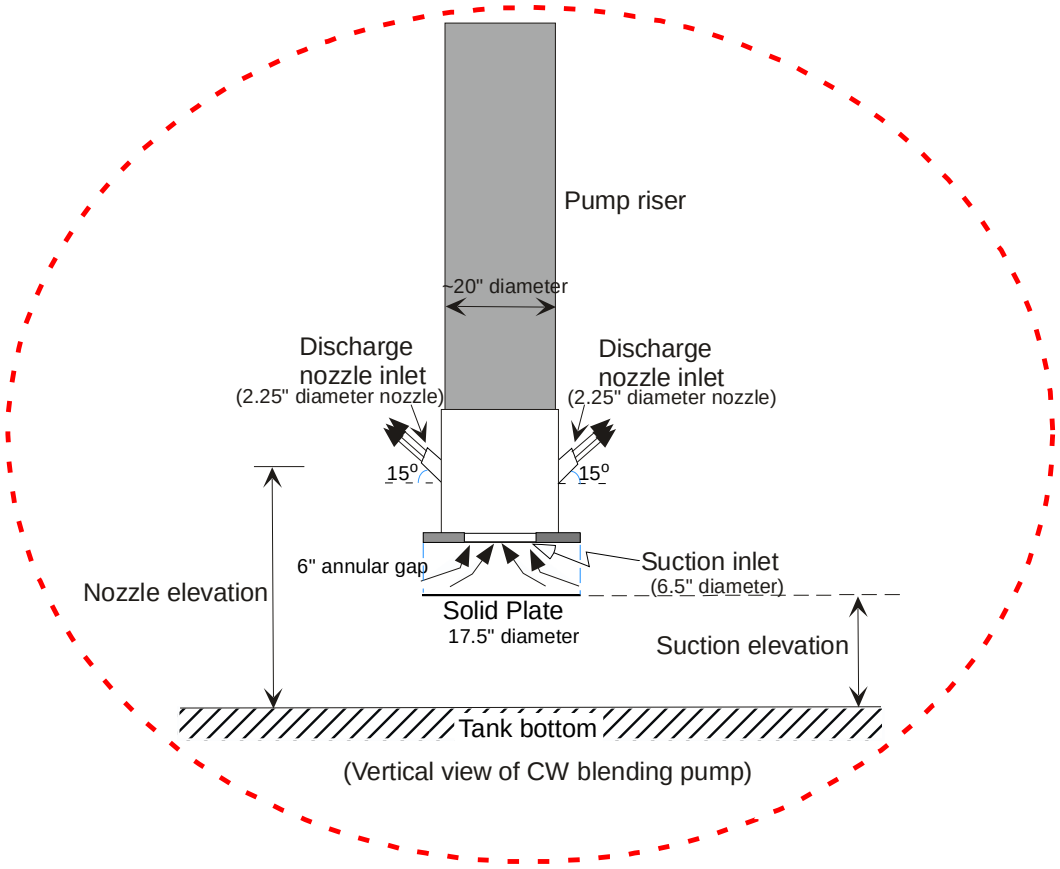

Figure 4. Geometrical configurations for the CW blending pump used in the phase-II final performance analysis

.Table 2. Modeling cases for the analysis

Cases	Description	Presence of cooling coils	Pump	Feed / Inj. fluids	$U_o d_o$	Purpose
Case1	EDL scale tank	No	T-shape (0.209")	Water/ Acid	0.81	Benchmarking / blending test / velocity / wall surface on tank bottom
Case2	EDL scale tank	No	T-shape (0.209")	Nitrate / Acid	0.81	Benchmarking / blending test / velocity, blending time / wall surface on tank bottom
Case 3	EDL scale tank	Yes	T-shape (0.209")	Water/ Acid	0.81	Benchmarking / blending test / velocity, sodium concentration, blending time / wall surface on tank bottom
Case 4	EDL scale tank	Yes	T-shape (0.209")	Nitrate/ Acid	0.81	Benchmarking / blending test / velocity, blending time / wall surface on tank bottom
Case 5	EDL scale tank	No	T-shape (0.209")	Water/ Acid	0.47	Benchmarking / blending time / wall surface on tank bottom
Case 6	EDL scale tank	Yes	T-shape (0.209")	Water/ Acid	0.47	Benchmarking / blending time / wall surface on tank bottom
Case 7	Full scale tank	No	T-shape (2.25")	Water/ Acid	8.8	Estimate blending time/sludge disturbance. Validate scale up techniques / wall surface on tank bottom
Case 8	Full scale tank	Yes	T-shape (2.25")	Water/ Acid	8.8	Estimate blending time. Validate scale up techniques / wall surface on tank bottom
Case 9	Full scale tank	Yes	T-shape (2.25")	Nitrate/ Acid	8.8	Estimate blending time / wall surface on tank bottom. Evaluate scale up effects of viscosity
Case 10	EDL scale tank	No	V-shape (0.209")	Nitrite/ Acid	0.47	Benchmarking / sludge mixing test / 7/8" slip plane on sludge surface, acceptance criteria for velocity
Case 11a	EDL scale tank	No	CW, parallel suction	Nitrate/ Acid	0.58	Estimate blending time / wall surface on tank bottom. Comparison to EDL blending time

Table 2. Modeling cases for the analysis (Continued)

Cases	Description	Presence of cooling coils	Pump	Feed / Inj. fluids	$U_o d_o$	Purpose
Case 11b	EDL scale tank	No	V-shape	Nitrite/ Acid	0.58	Benchmarking / sludge mixing test / 7/8" slip plane on sludge surface, acceptance criteria for velocity
Case 12a	EDL scale tank	Yes	V-shape (0.209")	Nitrate/ Acid	0.70	Estimate blending time / wall surface on tank bottom
Case 12b	EDL scale tank	Yes	CW , parallel suction	Nitrite/ Acid	0.70	Benchmarking / sludge mixing test / 7/8" slip plane on sludge surface
Case 13	Full scale tank	No	CW, parallel suction	Nitrate/ Acid	6.3	Sludge disturbance / 9.49" slip plane
Case 14	Full scale tank	Yes	CW, parallel suction	Nitrate/ Acid	7.6	Estimate blending time / wall surface on tank bottom
Case 15	EDL scale tank	No	Transfer pump with no solid plate	Nitrite	1.1 gpm	Benchmarking / flow patterns, estimate pump elevation. Pump location 3/4" above sludge yielded minimal sludge disturbance. 9/16" above sludge yielded some disturbance. CFD model for the bottom of the transfer pump (tubing) will be located at 9/16" above the sludge surface.
Case 16a	EDL scale tank	No	Transfer pump with solid plate, model	Nitrite	1.1 gpm	Benchmarking / flow patterns, estimate pump elevation. Pump location 3/8" above the sludge surface yielded minimal sludge disturbance. CFD model for the bottom of the transfer pump's bottom plate will be located at 3/8" above the sludge surface
Case 16b	EDL scale tank	No	Transfer pump with solid plate, model	Nitrite	1.1 gpm	Benchmarking / flow patterns, estimate pump elevation. Pump location 1/4" above the sludge surface yielded increased sludge disturbance. CFD model for the bottom of the transfer pump's bottom plate will be located at 1/4" above the sludge surface

Note: Wall surface on the tank bottom was modeled as no-slip boundary.

Table 2. Modeling cases for the analysis (Continued)

Cases	Description	Presence of cooling coils	Pump	Feed / Inj. fluids	$U_o d_o$	Purpose
Case 16b	EDL scale tank	No	Transfer pump with solid plate, model	Nitrite	1.1 gpm	Benchmarking / flow patterns, estimate pump elevation. Pump location 1/4" above the sludge surface yielded increased sludge disturbance. CFD model for the bottom of the transfer pump's bottom plate will be located at 1/4" above the sludge surface
Case 17a, 17b, 17c	Full scale tank	No	CW Transfer pump with solid plate	Nitrite	130 gpm	Estimate pump elevation and determine suction velocity under full-scale transfer pump. Elevation 5.43" sludge clearance. Investigations of other elevations may be added to the work scope, if required. (See Table 1)
Case 18	Full scale partial model	Yes	T-shape (0.209")	Water	Variable	Study of flow obstruction effects due to the presence of coil coils
Case 19	Full scale EMD model	Yes	V-shape (2.25")	Nitrate / Acid	6.1	Estimate blending time for full-scale CW pump with wall surface on tank bottom.
Case 19a	Full scale EMD model	Yes	V-shape (2.25")	Nitrate / Acid	6.1	Full-scale CW pump model with 9.49" slip plane.
Case 20	Full scale EMD model	No	V-shape (2.25")	Nitrate/ Acid	5.1	Estimate blending time for full-scale CW pump with wall surface on tank bottom.
Case 20a	Full scale EMD model	No	V-shape (2.25")	Nitrate/ Acid	5.1	Full-scale CW pump model with 9.49" slip plane.

Note: Wall surface on the tank bottom was modeled as no-slip boundary.

Table 3. Transfer pump models for different transfer pump configurations and elevations under EDL pilot-scale and full-scale operations

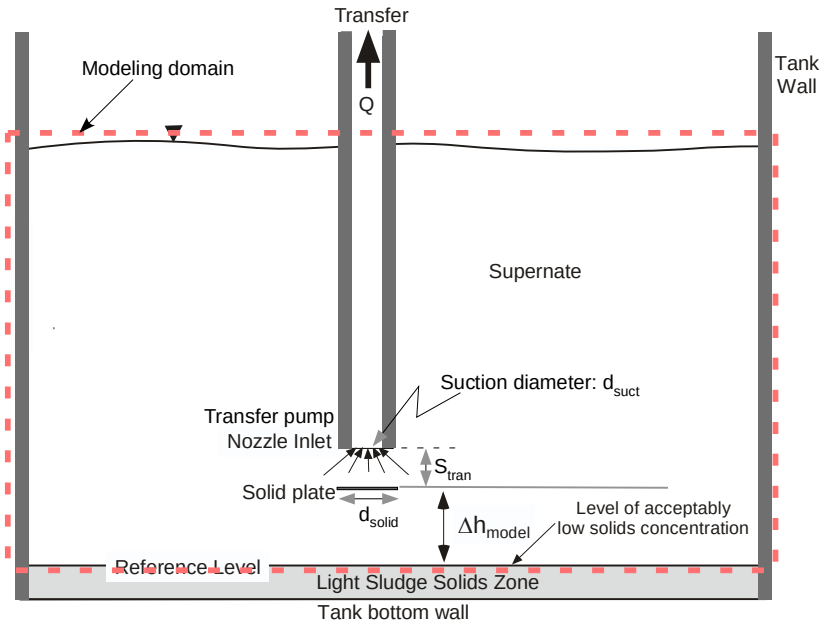

Case	Tank scale	Q (gpm)	d_{suct} (inches)	S_{tran} (inches)	d_{solid} (inches)	Δh_{model} (inches)
15	Pilot	1.1	0.221	0	0	9/16
16a	Pilot	1.1	0.221	0.37	1	3/8
16b	Pilot	1.1	0.221	0.37	1	1/4
17a	Full scale	130	2.4	6	18	5.43
17b	Full scale	130	2.4	2	11	9.5
17c	Full scale	130	2.4	4	10.85	5.43

Note: Use same % opening for the Transfer Pump suction screen, except that it is only 4 inches high.

3.0 LITERATURE REVIEW ON JET MIXING STUDIES

3.1 General Review

Mixing is usually carried out to obtain a uniform mixture, and it can be achieved using mechanical agitators, fluid jet mixers, and static mixers or multiple T-junctions. This work is concerned with the mixing issues driven by a turbulent jet. In jet mixing, a fast stream of liquid is discharged into a stationary bulk liquid. The relative velocity between the jet region and the bulk liquid creates a turbulent mixing layer via the formation of turbulent eddies at the jet boundary as illustrated in Fig. 3.

The literature results [Abramovich, 1963, Lee et al., 2004] show that when a turbulent jet of fluid is discharged from a nozzle into a stagnant fluid medium, it both entrains fluid and expands. The fluid domain for a large-scale tank has both a solid wall boundary and a free surface boundary as the jet expands into the downstream region and ultimately recirculates via the suction on the bottom of the pump. The spreading fluid is retarded by the interaction with the wall as shown in Fig. 5, and the inner part of the flow may be expected to show a certain structural similarity to a boundary layer. Entrainment of quiescent fluid occurs near the outer edges of the flow, and accordingly resembles a free jet [Abramovich, 1963]. In this case sludge particles near the edge of the jet plume are entrained into a turbulent zone, and they are suspended. Estimations of minimum suspension velocity, particle settling rate, and incipient erosion velocity have been performed to support the use of a computational fluid dynamics (CFD) approach to establish and evaluate a sludge mixing criterion in the previous work [Lee et al., 2008].

Most mixing action and entrainment takes place in the region of fully-developed flow which begins at a distance of approximately eight nozzle diameters from the exit plane [Abramovich, 1963]. From the reference [Abramovich, 1963], when a turbulent jet of fluid is discharged from a nozzle with a diameter d_o into a quiescent fluid, the non-dimensional velocity distribution, φ_v, along the jet axis for a homogeneous fluid is approximated by

$$\varphi_v = \left(\frac{v(x)}{U_o}\right) = C_o\left[\frac{x}{d_o}\right]^{-1} = C_o[\eta]^{-1} \qquad (1)$$

In Eq. (1), C_o is a constant determined by the turbulence characteristics of the jet, U_o the nozzle exit velocity, *v(x)* the local velocity at a point *x*, and *x* the distance from the nozzle. Abramovich (1963) correlated experimental data for a free turbulent jet submerged in fluid using the non-dimensional form provided by Eq. (1). From his work for free jet without any flow obstructions, the proportionality constant C_o in Eq. (1) was determined to be 6.32. Since the pump discharge flow inside the large-scale tanks at SRS is affected by the bottom of the tank and internal flow recirculation, the constant C_o is evaluated from previous Tank 18 calculations rather than classical free jet theory. It was found to be 4.874 [3]. The maximum axial velocity at any axial position *x* in an SRS waste tank can then be estimated using Eq. (1). The equation shows that the velocity at any point in the region of established flow is directly proportional to the product, $U_o d_o$. The axial entraining distance corresponding to the minimum entrainment velocity can be estimated with nozzle diameter and flow rate.

In the free turbulent jet experiment, the only non-dimensional parameter is the jet's Reynolds number, Re_{jet}. The dependency of the following parameters on Re_{jet} needs to be examined:

- The similar radial velocity profiles along the principal discharge direction
- Velocity decay constant (C_o)
- The spreading rate (R_s) defined by $r_{1/2}(x)/(x-x_o)$

Mean flow profile and the spreading rate are independent of Re_{jet} as shown in Table 4. However, it is evident the Reynolds number does affect the flow in terms of turbulent characteristics; such as, local entrainment behavior. The virtual origin is denoted by x_o, and the local half-width of the jet by $r_{1/2}(x)$. In the self-similar region (x/d > 40 [Bradbury, 1965]) of high Reynolds number turbulent jets (Re_{jet} > 10,000), the centerline velocity U_{max} and the half width $r_{1/2}$ are linearly proportional to the separation distance from the jet exit.

Fluid entrained in the jet region is transported and dispersed across it by motion induced from the largest to the smallest eddies. Eckart (1948) demonstrated that turbulent jet mixing can be viewed as a three-stage process of entrainment, dispersion (or stirring), and diffusion, spanning the full spectrum of space-time scales of the flow. In liquids, where species mass diffusivities are much smaller than kinematic viscosities resulting in a large Schmidt number (ratio of kinematic viscosity to mass diffusion coefficient), it is useful to split the diffusive action into two steps, one in which viscosity acts with acquisition of small-scale vorticity and the second where mass diffusion takes place. A mixed blending condition is reached at the time when a continuous liquid phase contains a spatially uniform composition of the discontinuous phase over the entire liquid domain of the tank within 95% homogeneity.

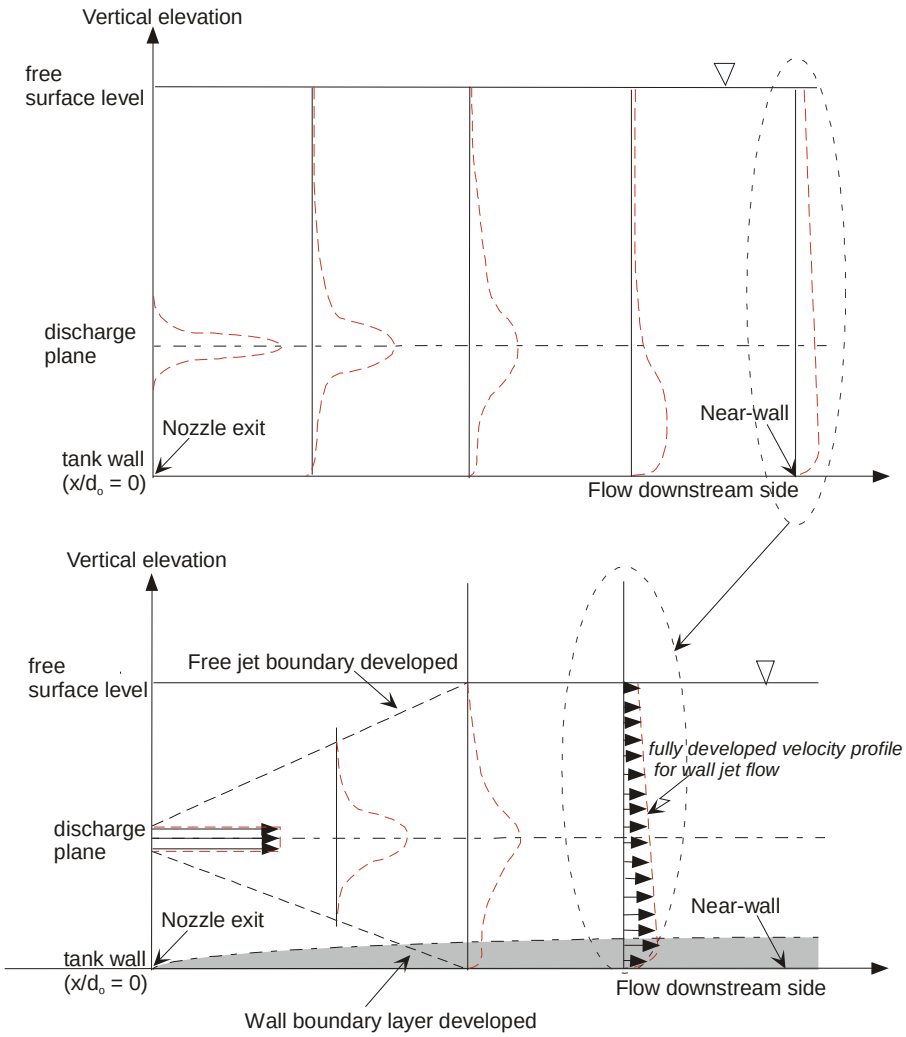

Figure 5. Typical velocity profiles in the direction perpendicular to the free surface from the previous modeling results of large-scale tank mixing simulations [Lee et al, 2008].

Table 4. Velocity decay constant and spread rate for free turbulent jets

Authors (year)	Re_{jet}	Decay constant (C_o)	Spreading rate (R_s)
Abramovich (1963)	20,000 - 4,000,000	6.31	---
Kiser (1963) (Conductivity cell data)	35,000	6.1	0.085
Rushton (1980)	5,600 – 200,000	$1.41Re_{jet}^{0.135}$	---
Panchapakesan & Lumley (1993)	11,000	6.06	0.096
Hussein et al. (1994) (Hot-wire data)	95,500	5.90	0.102
Hussein et al. (1994) (Laser-doppler data)	95,500	5.80	0.094

This mixing layer grows in the direction of the jet, entraining and mixing the jet liquid with the stagnant bulk liquid. Based on this concept, it has been assumed that longer jet lengths result in better mixing performance. The jet length, L, in the literature has been defined as the maximum distance a jet travels before it impinges on the opposite wall. For a cylindrical tank, the longest jet occurs when a jet is discharged at the bottom of the tank diagonally upward toward the opposite side. Thus, most researchers, including Grenville and Tilton (1996, 1997), have considered an inclined injection angle of about 45^o for their experimental investigations to quantify mixing performance and time.

Various techniques have been employed by researchers to examine the mixing behavior of a jet in an attempt to achieve a fundamental understanding of turbulent mixing. These include optical techniques and conductivity measurements. The experimental results for the mixed system have been proposed in the form of correlations to quantify the mixing time for a jet. These mixing correlations can be divided into two main categories. One is dependent on turbulence parameters; such as, turbulent kinetic energy, energy dissipation rate, and turbulent eddy viscosity, although they are not easily measurable or quantifiable. The other is dependent on measurable quantities; such as, tank geometrical dimensions, and jet flow conditions. However, all of the literature correlations are basically related to two primary parameters, a geometrical length scale and the turbulent eddy viscosity.

Fossett and Prosser (1949) used a conductivity technique to measure mixing time for a turbulent jet. Their correlation contains tank diameter, jet diameter, and jet exit velocity. It is independent of the jet Reynolds number and does not include the effect of kinematic viscosity on the mixing time. It is applicable to the range of jet Reynolds numbers, 4,500 to 80,000. Many other researchers developed a similar correlation as shown in Table 5.

Fox and Gex (1956) indicated that mixing time is dependent on the jet Reynolds number. The Reynolds number is defined in terms of propeller diameter and speed. As jet flow is changed from laminar (Re = 300) to the turbulent flow regime (Re = 150,000), its dependence on the jet Reynolds number becomes weaker.

Lane and Rice (1982) investigated liquid jet mixing employing an inclined side entry jet. In their experimental study, conductivity measurements for tracer concentration were made at a monitoring point at any time to estimate the mixing time. They studied two designs for inclined side entry jet mixing, and they correlated their data to develop a general expression for mixing time in terms of measurable parameters; such as, jet velocity, tank dimensions, and fluid properties. They proposed a correlation for jet mixing time to predict the time required to achieve a 95% degree of mixing throughout the tank using an inclined jet located at the side entry near the tank bottom. For C_{eq} the equilibrium concentration and C the transient concentration at a monitoring point, the 95% mixing time t_m was defined by

$$t_m = \left| \frac{C - C_{eq}}{C} \right| < 0.5 \qquad (2)$$

Their correlation has a mixing time factor, *F*, and the factor is a function of the jet Reynolds number, which is similar to the friction factor associated with the momentum dissipation. It is noted that the F factor exhibits two different trends in the laminar and the turbulent regions as shown in Table 5. As discussed earlier, its dependence on jet Reynolds number is significant in the laminar region, and weak in the turbulent regime.

A number of experimental studies have been carried out to investigate the flow patterns associated with jet mixing. Maruyama et al. (1982) reported mixing times for horizontal jets, inclined jets toward top free surface, and jets vertical to tank floor. In this case, jet was located near the corner of tank floor. They proposed that the mixing time is a function of Reynolds number and jet length, but they emphasized the role of the flow patterns inside the tank on the mixing time behavior.

Perona et al. (1998) performed mixing experiments with water in two different scales of tanks. They are 2 ft in diameter by 10 ft in length (230 gallons) and 10 ft in diameter by 40 ft in length (25,000 gallons). The smaller one was about 1/6 linear scale of the actual storage tanks and was made of Plexiglas to permit flow visualization studies. Data were taken with a single jet placed about a quarter tank length from one end pointed horizontally towards the center of the tank. The jet nozzles were straight pieces of pipe, and their diameter and velocity were varied with this configuration. Jet diameters of 0.62, 0.87, and 1.61 inches were tested with the jet located 1.25 inches above the tank bottom for the two smaller diameters, and 1.75 inches above the floor for the largest-diameter jet in each of the two tanks. Tests were made with two-directional opposed jets along the same axis at this location, and at the center of the tank lengthwise. In all cases, the jet was positioned close to the bottom of the tank, in the range of 1 to 4 jet diameters from the floor to the jet centerline. They measured jet mixing times for long horizontal tanks with length-to-diameter ratios of 4 and 5. Mixing times in the 230 gallon tank decreased from 1800 seconds to 300 seconds as the jet Reynolds number was increased from 15,000 to 130,000. With a single jet in the 25,000 gallon tank, mixing times decreased from 4500 to 840 seconds as the jet Reynolds number was increased from 80,000 to 311,000. For two-opposing jets of the same diameter and location, mixing times were not significantly different from those of the single jet at the same flow rate. At a given flow rate, mixing

times were significantly lower with a 1.38-in double jet than with a 1.93-in double jet. They found that about 28 tank volumes must be recirculated through the entrained jet for good mixing with tanks of this configuration. Their empirical correlation for mixing time is shown in Table 5.

Grenville and Tilton (1996) investigated the mixing process by giving a pulse of tracer (electrolyte) through the jet nozzle and by monitoring the conductivity at three locations within the tank. They proposed that the mixing process was controlled by the turbulent kinetic energy dissipation rate in the region far away from the jet entrance. They took the energy dissipation rates in the regions remote from the nozzle to be proportional to jet velocity at that location, and jet diameter. The reduction in the jet velocity was taken to be proportional to the nozzle velocity and distance from the nozzle. Based on this analysis, a correlation was proposed. The proposed correlation was shown to be valid over a wide range of Reynolds numbers with a relative standard deviation of $\pm$11.83%.

An improved correlation including the effect of circulation time was proposed by Grenville and Tilton (1997) via a better fit of mixing time data for turbulent jet mixing under a wider range of jet Reynolds numbers (50,000 to 300,000). The circulation time was defined as the liquid volume divided by the entrained flow rate. They assumed that the mixing rate at the end of the jet length controls the mixing time for the entire tank by estimating the kinetic energy dissipation rate as discussed earlier. They predicted that for a given volume, an optimum geometry exists for a mixing vessel, allowing a desired mixing time to be achieved for a minimum power input. This optimum condition occurs when the aspect ratio of the tank height to diameter is $2^{-0.5}$. The current work will compare the Grenville and Tilton (1997) correlation of the jet mixing time with CFD modeling results for their experimental tanks in an attempt to achieve a fundamental understanding of the turbulent jet mixing, and to establish mixing indicators.

3.2 Basic Characteristics of Turbulent Jet Mixing / Blending

Equation (1) indicates that the velocity at any point in the region of established flow is directly proportional to the product, $U_o d_o$. Thus, the one-dimensional entraining distance corresponding to minimum entrainment velocity can be estimated theoretically when nozzle size and pumping flowrate are provided. However, the fluid region for the present work has both a solid boundary and a free surface boundary as the jet expands into the downstream region; and then, the flow recirculates in the tank. The spreading fluid is retarded by the frictional resistance of the wall, and the inner part of the flow may be expected to show a certain structural similarity to a boundary layer; whereas, entrainment of quiescent fluid occurs near the outer edge of the flow which is likely to resemble a free jet in character.

When a solid structure or wall surface is present near the jet nozzle, the jet flow will react to a three-dimensional interaction from the wall boundary and free surface. The literature results [Abramovich, 1963] showed that the flow region of the jet up to 40 nozzle diameters, η = 40 in Eq. (1) was not affected by the presence or absence of a wall near the nozzle. The results for the region farther than 40 diameters [Abramovich, 1963; Chadrasekhara Swamy and Bandyopadhyay, 1975] show that the velocity along the axis of a jet, which is expanding along a wall in an accompanying flow, dies out more quickly than in the analogous free jet.

3.3 Review Summary

The literature review on the quantitative measurement and evaluation of flow entrainment by a jet stream, and the time required to reach a certain degree of homogeneity have been performed to investigate key turbulent parameters for use as mixing performance indicators. The literature reviews on turbulent jet mixing analysis are summarized as follows:

- Jet flow evolution plays a significant role in jet mixing; including, jet nozzle orientation inside the tank, range of jet Reynolds numbers, and a recirculation effect coupled with the geometrical aspect ratio of liquid depth to tank diameter.
- Mixing time is dependent on Reynolds number, and scale ratios. For mixing operations with high Reynolds number, the mixing time is dependent primarily on scale ratios.
- Mixing time for a large volume tank is not affected by the angle of nozzle inclination.
- Most literature results are limited to high depth of liquid above the jet location since no vortex formations were observed at the top liquid surface. Thus, the effect of Froude number referred to the nozzle was neglected in correlating the mixing time.

Table 5. Models and correlations for mixing time

Model	Authors	Mixing time	Validity
Empirical model	Grenville and Tilton (1996)	$3.0\left(\frac{L}{d_o}\right)^2\left(\frac{d_o}{U_o}\right)$	(50,000 < Re_{jet} < 300,000)
Empirical model including the effect of circulation time	Grenville and Tilton (1997)	$S\left(\frac{D^2}{U_o d_o}\right)\left(\frac{h_l}{L}\right)$, where S = 9.34 for θ > 15°, and S = 13.8 for θ < 15°.	(50,000 < Re_{jet} < 300,000) The parameter θ in their correlation is inclination angle of the jet nozzle and the horizontal.
Empirical model	Fossett and Prosser (1949)	$\frac{9.0D^2}{U_o d_o}$	(4,500 < Re_{jet} < 80,000)
Empirical model	Fox and Gex (1956)	$\frac{f_{jet} h_l^{0.5} D}{(U_o d_o)^{4/6} g^{1/6}}$ (f_{jet} = f (Re) for jet mixing)	(270 < Re_{jet} < 155,000)
Empirical model	Perona et al. (1998)	$C\left(\frac{V_T}{Q_j}\right)\left(\frac{d_o}{L}\right)$, where the constant C is about 28 from data.	Long horizontal tank for d_o = 0.6m, H = 3m, d = 16, 22, 41 mm (including two opposing horizontal jets)
Empirical model	Okita and Oyama (1963)	$5.5\left(\frac{h_l}{D}\right)^{0.5}\left(\frac{D}{d_o}\right)^2\left(\frac{d_o}{U_o}\right)$	Inclined side entry jet (5,000 < Re_{jet} < 100,000)
Empirical model	Lane and Rice (1982)	$F\left(\frac{h_\ell^{0.5} D}{(U_o d_o)^{0.667} g^{0.166}}\right)$, where F = $C_1(Re_{jet})^{-1.133}$ for laminar flow and $C_2(Re_{jet})^{-0.166}$ for turbulent flow	(200 < Re_{jet} < 100,000)
Dispersion model (G. I. Taylor)	Fischer (1973)	$C\left(\frac{\lambda^2}{\nu_t}\right)$	The constant C is dependent on flow conditions.
Eddy dissipation model	Spalding (1971)	$\left(\frac{k}{\varepsilon}\right)$	High Re (fully turbulent region)
Engulfment model	Baldyga and Bourne (1984)	$C\left(\frac{\nu_t}{\varepsilon}\right)^{0.5}$	High Re (fully turbulent region) The constant C is dependent on flow conditions.

4.0 MODELING APPROACH AND ANALYSIS

For the present analysis, a three-dimensional computational fluid dynamics (CFD) approach was taken to calculate flow velocity distributions, and to estimate blending time for two miscible liquids; such as, salt solution and acid, for Tank 50 as illustrated in Fig. 6. The results are benchmarked against both EDL-scale test data and literature data. The commercial finite volume code, FLUENT, was used to create a full scale geometry file in a non-orthogonal mesh environment.

The model geometry was created using the body-fitted coordinate system and structured multi-block grids. For the blending performance analysis, the reference design conditions were considered as shown in Fig. 1 and Table 1. The blending pumps (T- and V-shape) for the EDL experiment are submerged inside a cylindrical tank that is 40 in high and about 94 in diameter. This tank corresponds to 1/10.85 scale with respect to the full scale of Tank 50. The nozzle size was scaled down to 0.209 in linearly from 2.25 in full scale pump nozzle. All of the models were developed for the nozzles installed at the mid-elevation and parallel to the tank wall as shown Fig. 6.

For the modeling calculations, the transient governing equations consisting of one mass balance, three momentum equations, two turbulence transport equations for kinetic energy (k) and dissipation rate (ε), and one species transport were solved by an iterative technique until the species concentrations of tank fluid were reached at equilibrium concentration within 5% relative error. The steady-state flow solutions for the entire tank fluid were used for the initial conditions.

In the present analysis, top tank liquid surface was assumed to be frictionless for computational efficiency, neglecting the detailed wave motion of the free surface. That behavior does not have a significant impact on the flow patterns inside the slurry region in a deep tank. The fluid properties of water or salt solution were evaluated at constant temperature (20^{o}C). The flow conditions for the pump operations are assumed to be fully turbulent since Reynolds numbers for typical operating conditions are in the range of 5 x10^4 to 1.0 x10^6 based on the pump nozzle inlet conditions. A standard two-equation turbulence model, the κ–ε model [Lee and Dimenna, 1995], was used to capture the turbulent flow evolution driven by the blending jet pumps since previous work [Lee et al., 2008] showed that the two-equation model predicts the flow evolution of turbulent jet in a large stagnant fluid domain with reasonable accuracy. This model specifies the turbulent or "eddy" viscosity ν_t by the empirical equation.

$$\upsilon_t = \frac{\mu_t}{\rho_f} = \left(\frac{C_\mu k^2}{\varepsilon} \right) \tag{3}$$

In Eq. (3), C_μ is an empirical constant. In the present calculations, C_μ is 0.09. Thus, the turbulent viscosity is computed by solving two transport equations for k (turbulent kinetic energy), and ε (rate of dissipation of turbulent energy).

From these two key parameters of k and ε, a lengthscale ($k^{1.5}/\varepsilon$), a timescale (k/ε), a quantity of turbulent eddy diffusivity (k^2/ε), can be formed without specification of flow-dependent mixing lengthscale λ [Jones and Launder, 1972]. Turbulence kinetic energy (k) is the mean kinetic energy per unit mass associated with eddies in turbulent flow.

Physically, the turbulence kinetic energy is characterised by measured root-mean-square (rms) velocity fluctuations. In the Reynolds-averaged Navier Stokes equations, the turbulence kinetic energy can be calculated based on the closure method, i.e. a turbulence model. Generally, the turbulent kinetic energy can be quantified by the mean of the turbulence normal stresses:

$$k = \frac{1}{2}\left\{\overline{(u_x)^2} + \overline{(u_y)^2} + \overline{(u_z)^2}\right\} \tag{4}$$

k can be produced by fluid shear, friction or buoyancy, or through external forcing at low-frequency eddie scales (integral scale). Turbulence kinetic energy is then transferred down the turbulence energy cascade, and is dissipated by viscous forces at the Kolmogorov scale. This process of production, convective transport and dissipation as modeled for *k* transport balance in the two-equation turbulence model can be expressed as:

$$\frac{Dk}{Dt} = \nabla \bullet \left(\frac{\upsilon_T}{\sigma_k}\nabla k\right) + P - \varepsilon \tag{5}$$

The three other terms, -*Dk/Dt*, *P*, and ε, are in closed form given the turbulent-viscosity hypothesis.

Turbulence consists of high levels of fluctuating vorticity. At any instant, vortical motion called eddies are present in the flow. These eddies range in size from the largest geometrical scales of the flow; such as, tank diameter, down to small eddies where molecular diffusion dominates. The eddies are continuously evolving, and the superposition of their induced motions leads to the fluctuating waves. In this situation, turbulent kinetic energy is dissipated from the largest eddies down to the smallest through a process called energy cascade. In order to maintain the turbulence, a constant supply of energy must be fed to the turbulent fluctuations at the largest scales from the mean motions, where it is driven by a jet pump or mechanical agitator. Thus, turbulent energy dissipation rate ε is viewed as the energy-flow rate in the cascade, and it is determined by the large-scale motions, independent of the viscosity at high Reynolds number. Consequently, the transport equation for ε is best considered as being entirely empirical. That is,

$$\frac{D\varepsilon}{Dt} = \nabla \bullet \left(\frac{\upsilon_t}{\sigma_\varepsilon}\nabla \varepsilon\right) + C_1\left(\frac{\varepsilon}{k}\right)P - C_2\frac{\varepsilon^2}{k} \tag{6}$$

The governing equations to be solved for the present work are composed of one continuity equation, three momentum equations for the three component directions (x, y, and z directions), and two constitutive equations for the turbulence descriptions. The detailed descriptions for the governing equations and computational methods are provided in the previous work [Lee et al., 2008].

When a tracer species; such as, acid material, is added to the tank during blending operations before transfer of the tank contents, the added species is transported over the tank domain by the continuous fluid motion driven by the jet pump. The modeling calculations for the blending time require the balance equation of tracer species. The species balance equation is given by

$$\frac{\partial \rho Y_v}{\partial t} + \nabla \cdot (\rho \vec{v} Y_v) = -\nabla \cdot \vec{J}_v + S_v \quad (7)$$

Y_v is local mass fraction of tracer species in the continuous fluid. $\vec{J}_v$ is diffusion flux of tracer species. S_v in the equation is a source term of tracer species added to the tank fluid due to the injection of the acid from the top of tank. The diffusion flux of tracer under turbulent fluid flow is computed by

$$\vec{J}_v = -\left(\rho D_v + \frac{\mu_t}{Sc_t}\right)\nabla Y_v \quad (8)$$

D_v is molecular diffusion coefficient of tracer in the continuous fluid medium. Typical molecular diffusion coefficient of liquid species in the liquid domain is about 1×10^{-9}, which is much smaller than gas species.

The governing equations described above are solved over the entire tank domain with and without cooling coils as shown in Fig. 6. For the calculations, the domain was meshed by a hybrid meshing technique. Number of meshes for the domain with no cooling coils was established as about 1×10^6 nodes as shown in Fig. 7. The number of mesh nodes for the model with 560 cooling coils was about 4×10^6 through utilization of a custom mesh template. Figure 8 shows three-dimensional computational volume meshes and representative two-dimensional meshes near the pump and cooling coils for the tank model with cooling coils.

A blending model of the tank configuration was set up with the return path reflecting the actual EDL experimental configuration as described by Leishear et al. (2010). The modeling domain and configurations for the tanks without and with cooling coils are shown in Fig. 6. As shown in the figure, a dual jet pump with horizontal direction or 15^o upward angle is located at the middle elevation of the tank, and the jetted flow returns to the tank through the suction inlet. In this case, the species fluid was an acid of 1.14 specific gravity and 1.16 cp viscosity, and total volume injected through the 0.43 inch hole was about 0.32 gallons for the initial period of 11.5 seconds. The acid was injected at Riser 5 as schematically shown in Fig. 1. Detailed test configurations performed at EDL are provided in the recent report [Leishear et al., 2010]. The transient contaminant profile was then calculated and observed.

A series of the modeling calculations were performed to estimate the blending times for various jet flow conditions and to investigate the impact of the cooling coils on the blending time. Based the blending model, the calculations for two separate cases were performed. The first case is the transient calculations of the species concentration in a tank with no cooling coils. The second calculations are for the tank fluid with 560 cooling coils as built in Tank 50H. In each case, two different scale models of 1/10.85 EDL scale and prototypic Tank 50H were developed. The modeling results were benchmarked against the pilot EDL and full scale TNX scale test results. All detailed modeling conditions considered here are summarized in Table 2.

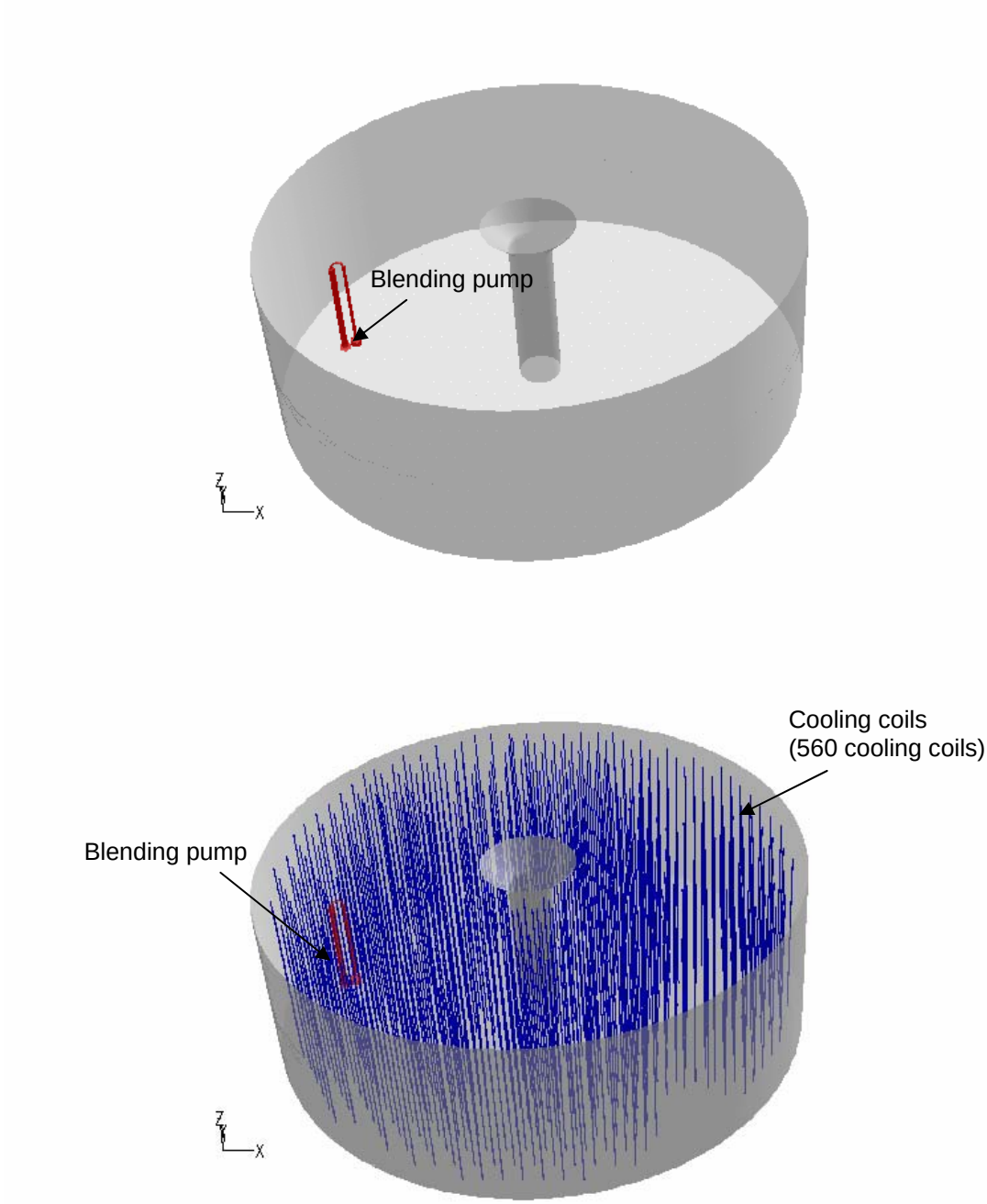

Figure 6. Computational domains of the tank models with and without cooling coils for the CFD analysis

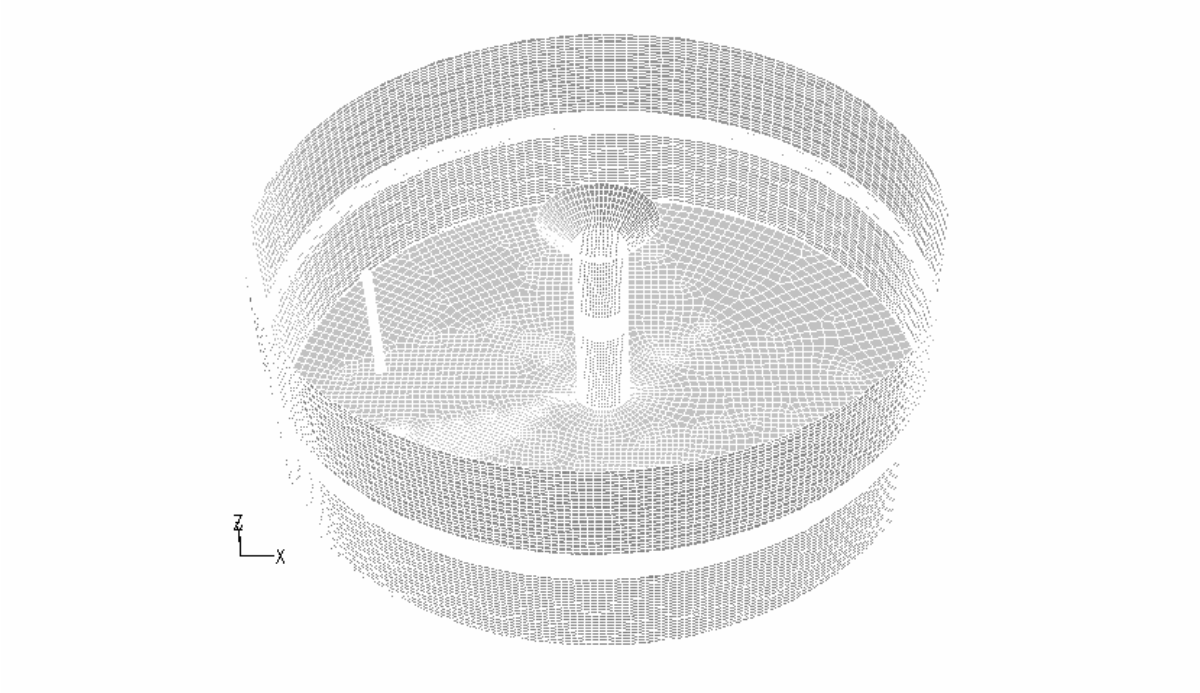

Figure 7. Three-dimensional view of computational volume meshes for the tank model with no cooling coils

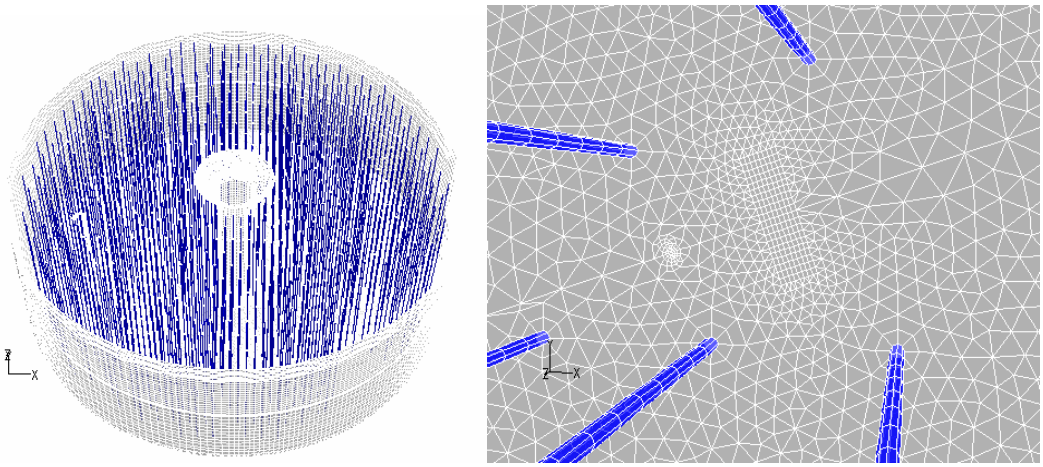

(Volume mesh for the tank with cooling coils)

(Cross-sectional representation of the refined mesh near pump and cooling coil surfaces)

Figure 8. Three-dimensional view of computational volume meshes and representative two-dimensional meshes near the pump and cooling coils for the tank model with cooling coils

5.0 RESULTS AND DISCUSSIONS

As shown in the literature review, jet flows contain irregular turbulent motions over a wide range of length and time scales. When a chemical tracer component introduced into the fluid is assumed to be mixed by the dissipation process of the turbulent energy, key operating parameters; such as, product of nozzle diameter, and jet discharge velocity, $U_o d_o$, are expected to provide a good indicator of mixing performance as shown in Table 5. The current turbulent flow simulations were mainly based on the k-ε model since the standard k-ε model is well known to be valid only for very large Reynolds number (i.e., greater than 10^5 Reynolds number).

Based the two-step approach, the modeling calculations were made for the numerical simulation as performed for the EDL blending tests. The first step is to establish the steady-state flow patterns of submersible jet flows as performed for the experiment. The second step is to perform the transient modeling calculations starting with another set of species balance equation in addition to the continuity, momentum, and two turbulence equations. In this approach, the transient calculations were started from the fully developed flow distribution of the first step steady-state runs as initial conditions. For the second step, a transient run was started with acid species injected into the fully-developed flow pattern established by the first step, and run until the acid species was mixed with continuous phase in a homogeneous way within 95%. A contaminant species started from the fully developed condition of the first step in which the species was injected for 11.5 seconds into the 0.43 inch hole at the top of the tank (Riser 5). In this case, the species fluid was an acid of 1.14 specific gravity and 1.16 cp viscosity, and total volume injected through the hole was about 0.32 gallons for the initial period of 11.5 seconds. Detailed test configurations of the EDL system are shown in Reference [Leishear, 2010]. The transient contaminant profile was calculated and observed.

The species added to the tank fluid is dispersed by the convective fluid motions established by the dual jet pump. The initial baseline calculations were based on the horizontal T-shaped dual jet pump, but after the 2nd phase test runs with a thin sludge layer settled on the tank floor, 15° V-shaped dual jet was required to ensure that the sludge layer would not be disturbed during the blending process of miscible fluids. Those two pumps are shown in Figs. 1 and 4, respectively. Figures 9 and 10 presents typical steady-state convective flow patterns established by the standard T-shaped dual jet pump, and the V-shape blending pump. The results indicate that the V-shaped pump has more active flow zone for the region above the pump elevation, resulting in the less momentum dissipation near the sludge region, when compared to that of the horizontal T-shaped one.

When the acid species is added into the steady-state flow patterns established by Case 1 operating conditions, the transient species concentrations at the pump discharge plane for Case 1 are shown in Fig. 11, noting that numbers in the color map indicate local concentrations non-dimensionalized by equilibrium value. The results clearly show that the species concentrations at the pump discharge plane are reached at equilibrium in about 4.2 minutes. It is indicated that the blending time over the entire domain of the tank fluid is about 4.6 minutes, showing the opposite lower region of the pump area has the longest blending time. This is consistent with the results observed by the test.

The benchmarking tests are chosen as two typical areas representing the turbulent jet dissipations, and flow dispersion behavior since these two phenomena are closely related to the miscible fluid blending, and sludge scouring mechanisms within the supernate space above the settled sludge layer. One is the momentum dissipation area directly impacted by the submerged jet parameter $U_o d_{o,}$ and the other one is the remote area indirectly influenced by forced convective circulation. Both of the benchmarking areas are closely related to the blending times of the miscible tank contents, and the scouring behavior of the sludge solids. The detailed results are provided in the subsequent section.

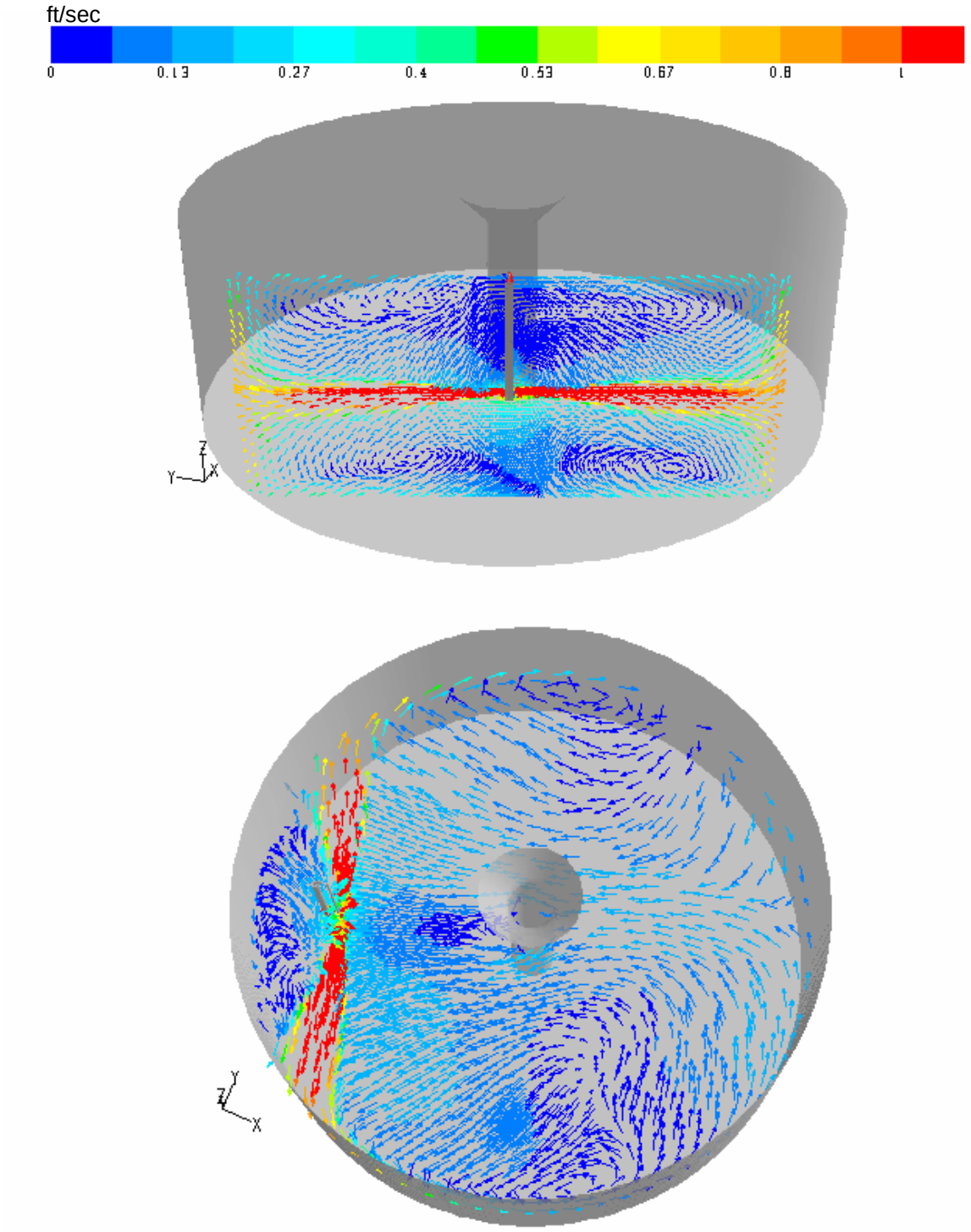

Figure 9. Typical flow patterns on the vertical and horizontal discharge planes of the T-shaped jet pump (Case 1)

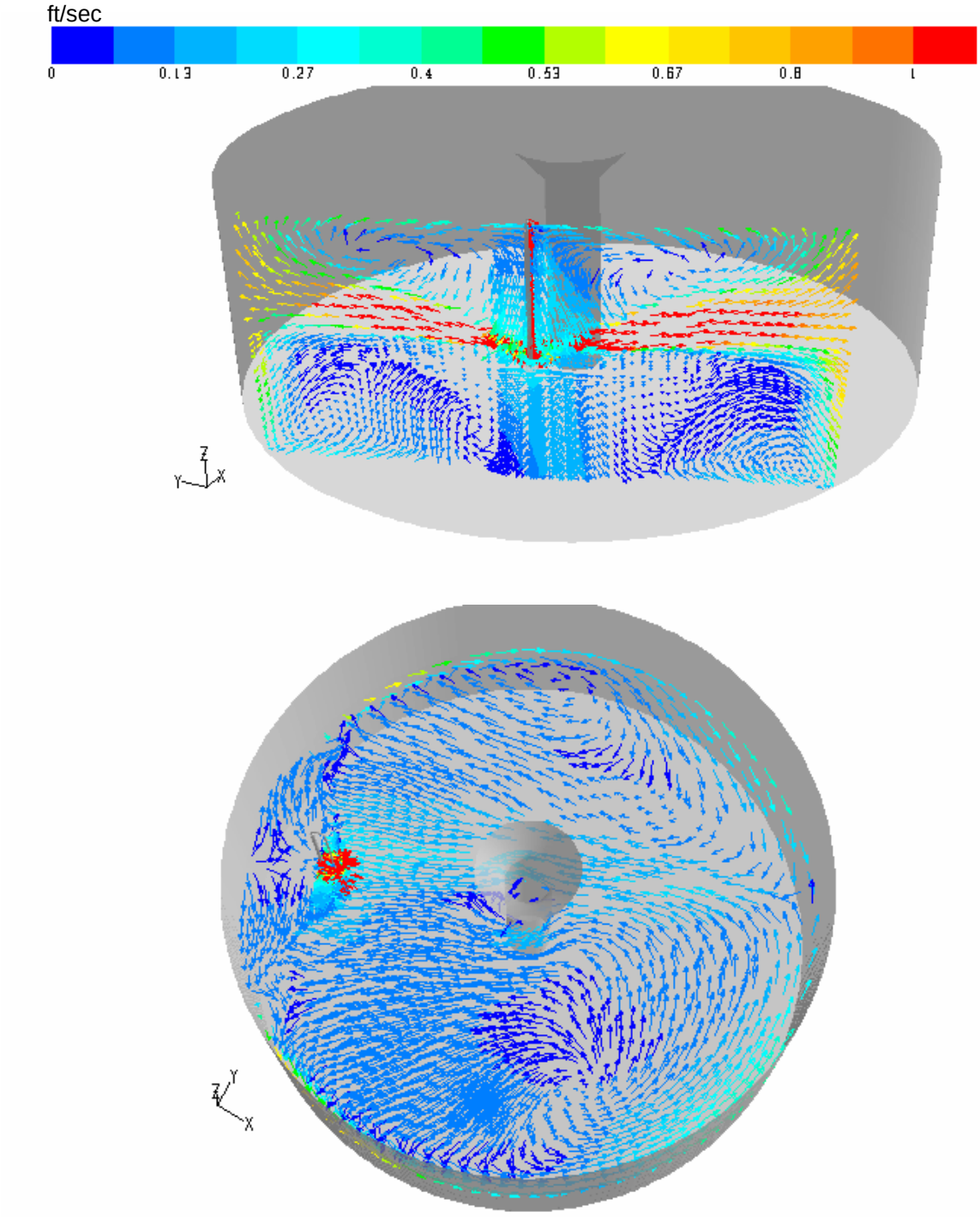

Figure 10. Typical steady-state flow patterns on the vertical and horizontal discharge planes of the V-shaped jet pump (Case 11a)

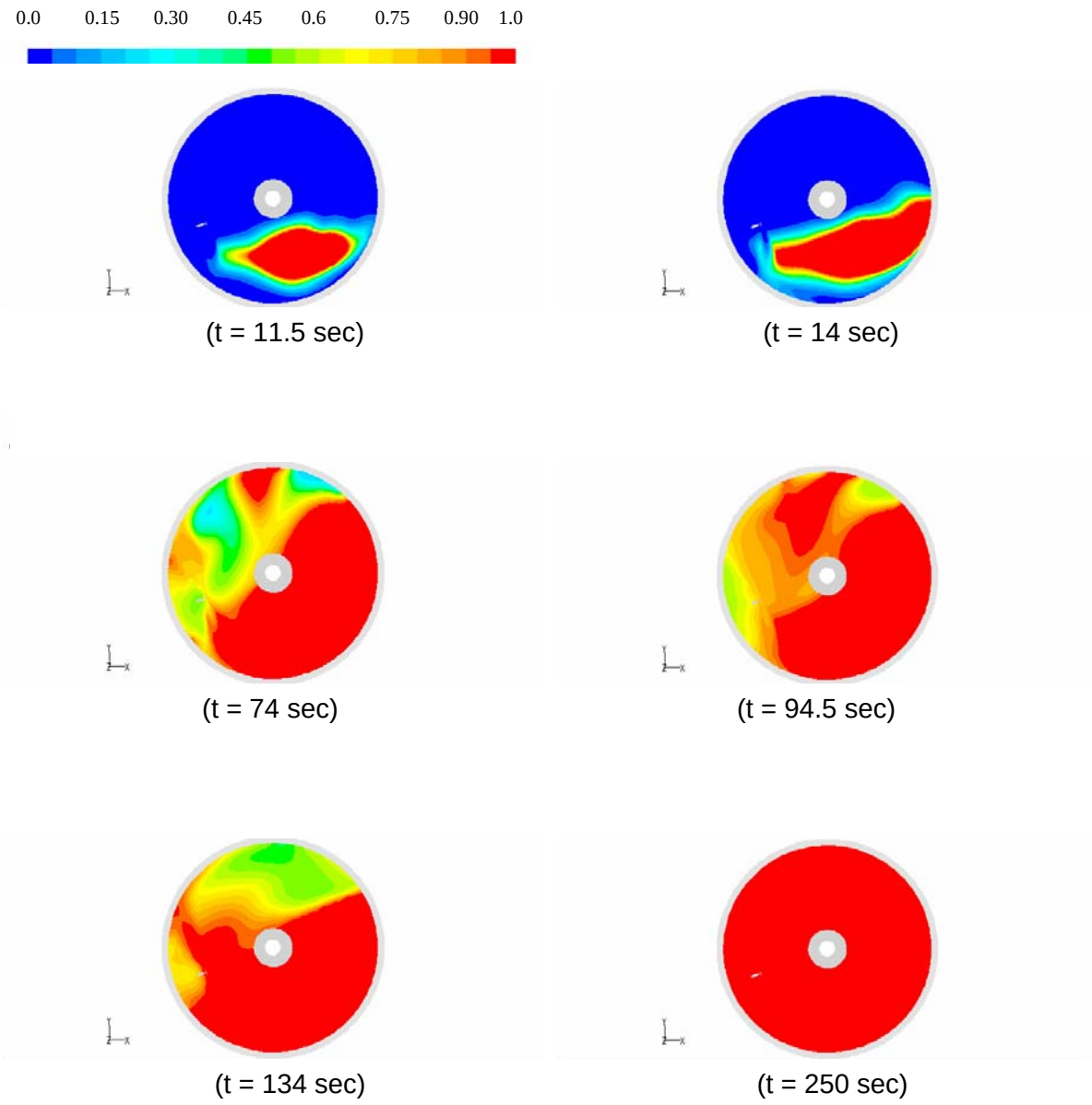

Figure 11. Transient tracer concentrations at the pump discharge plane for Case 1 showing that number in color map indicates the non-dimensionalized value with respect to equilibrium concentration.

5.1 Benchmarking Results

The benchmarking studies of the CFD models against local velocity measurements done for the EDL-scale tests were performed for the initial design requirements for a full scale blending pump. When a jet stream of liquid is discharged into a stationary bulk liquid, the relative velocity between the jet region and the stagnant bulk liquid creates a turbulent mixing layer via the formation of turbulent eddies at the jet boundary. Thus, the momentum dissipation rate is closely related to the blending time of miscible fluids. When the Case 1 blending pump is used inside the EDL scale tank with no coils, the steady-state flow evolutions of the blending jet along the principal discharge line are benchmarked against the literature results as shown in Table 6. The benchmarking results for local velocities along the jet discharge direction are shown in Fig. 12. The results demonstrated that the CFD model predicts the test results for a range of the jet operating conditions of $U_o d_o$ within about 20%.

Figure 13 shows positions for local velocity measurements on the tank fluid domain. As shown in the figure, four azimuthal locations, and four different elevations remotely away from the pump were chosen for the measurements of local velocities under the steady-state operating conditions. These measurements are for the benchmarking test of the CFD velocity criterion, which avoids disturbing the sludge layer settled on the tank floor. Figure 14 shows velocity flow patterns and local velocity measurement locations at 2 in elevation for the Case 1 modeling conditions. As shown in Table 7, quantitative comparison of the modeling predictions for local velocities is made to the test results for the local positions near the tank bottom under the Case 1 operating conditions of horizontal dual jet submerged in the water with $U_o d_o$ = 0.81 ft^2/sec. When the same $U_o d_o$ pump as Case 1 is operated for a heavier fluid content of Case 2, the modeling predictions are compared with the test results as shown in Table 8 and 9. All of these operating cases used the horizontal dual jet pump for the EDL-scale tests.

From the comparison of the flow patterns in Figs. 9 and 10, it is demonstrated that the both of 0^o T-shape and 15^o upward V-shape jet pumps have four vertical large circulation zones. The flow pattern results indicate that when the two pumps are operated under the same $U_o d_o$, the V-shaped pump has the stronger convective fluid motions with the smaller circulation zones for the two upper region above the pump discharge plane, compared to those of the two lower region, while the T-shaped pump has about the equal convective vertical circulation zones for those four regions with respect to the pump discharge plane. This is consistent with the experimental observations. A series of the pump performance studies has been performed to establish the optimum jet nozzle design, and maximum operating value of the jet $U_o d_o$ to prevent the sludge disturbance; as well as, the minimum value of $U_o d_o$ required for the adequate blending of the tank contents.

A pump with 15^o upward and V-shaped dual jets was established from the performance studies. The modeling results for the V-shape pump are compared to the EDL test results under $U_o d_o$ = 0.58 ft^2/sec as shown in Table 10 and Table 11. The comparative results for $U_o d_o$ = 0.70 ft^2/sec under the EDL-scale tank are shown in Table 12. All the CFD results for the local velocities are compared to the experimental results obtained by the 1/10.85 EDL-scale and full scale TNX tests in Fig. 15. The benchmarking results show that the CFD modeling predictions are in reasonable agreement with the test results within about 25% for a range of 1/10 EDL to prototypic TNX scales

From the modeling and experimental studies, the final pump design and operating conditions for the blending pump to satisfy those two criteria was established. Figure 4 presents the final pump with 15^o upward dual jets. The final operating conditions of U_od_o value to satisfy the two requirements of minimum sludge disturbance, and adequate blending of tank contents are established as 6.1 ft^2/sec for the tank with coils, and 5.1 ft^2/sec for the tank with no coils by considering the overall uncertainties.

The validated model was applied to the two different operating conditions of 0.81 ft^2/sec, Case 1, and 0.47 ft^2/sec, Case 5, under EDL scale tank in order to compare the size and location of the potential zones of sludge disturbance. The modeling results for the velocity distributions at the top surface of the sludge layer for those two jet conditions are shown in Fig. 16. Figure 17 compares the flow velocity distributions at the plane 1 inch above the tank floor for the EDL tank without and with cooling coils for 9.95 gpm, U_od_o = 0.81 ft^2/sec under the same color map. As shown in the figure, the modeling results show that local velocities near the tank bottom are reduced by about 15% due to the presence of the 560 cooling coils under the same U_od_o value. All the results show that both corner zones of the pump jets near the wall have the highest velocities regardless of the cooling coil presence. These results are consistent with the experimental observations.

The benchmark analyses for the CFD flow models demonstrate their consistency with EDL and literature test results in terms of local velocity measurements and experimental observations. Thus, an application of the established criterion to SRS full scale tank will provide a better, physically-based estimate of the required mixing time. When tracer species; such as, acid material, is added to the tank contents during blending operations before transfer of the tank contents, the added species is dispersed over the tank domain by the continuous fluid motion driven by the jet pump. The modeling calculations for the blending time require the transport equation for tracer species in Eq. (7), in addition to the turbulent flow equations. The modeling predictions for the blending times of the tank contents were benchmarked against the test results of EDL tank without and with coils. The benchmarking results for the cases without and with cooling coils are shown in Figs. 18 and 19, respectively.

Table 6. Data conditions of turbulent jets used in Fig. 12

Authors	U_od_o (ft^2/sec)	Jet diameter (mm)	Fluid	Reynolds number, Re_{jet}
EDL/SRNL (2010)	0.81	5.31	Water	75,000*
Kiser (1963)	0.38	9.525	Water	35,000
Post (1998)	1.62	10	Air	10,000

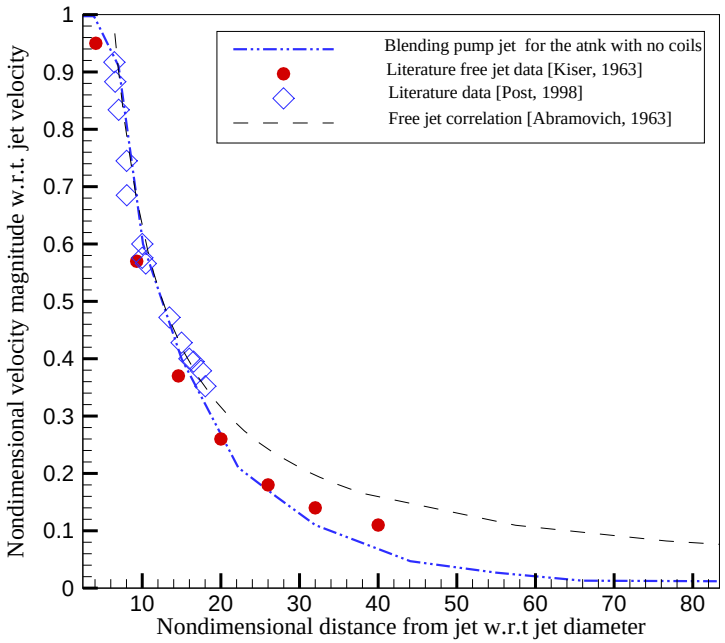

Figure 12. Comparison of steady state flow evolutions of the blending jet with the literature data along the principal discharge line inside the EDL scale tank with no coils

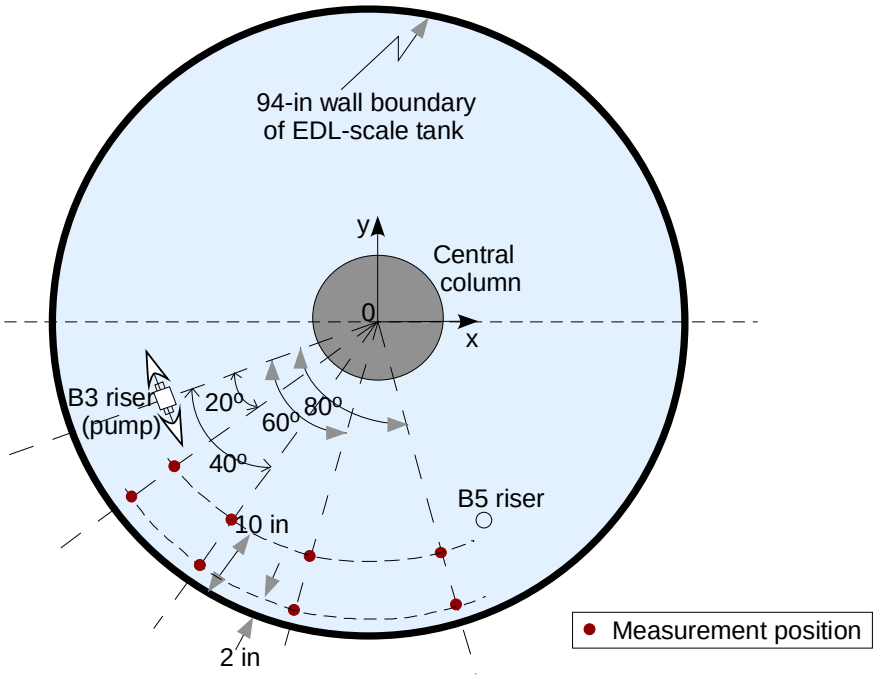

(Vertical positions from tank floor: 2, 4, 8, and 16 inches)

Figure 13. Positions for local velocity measurements on the tank fluid domain

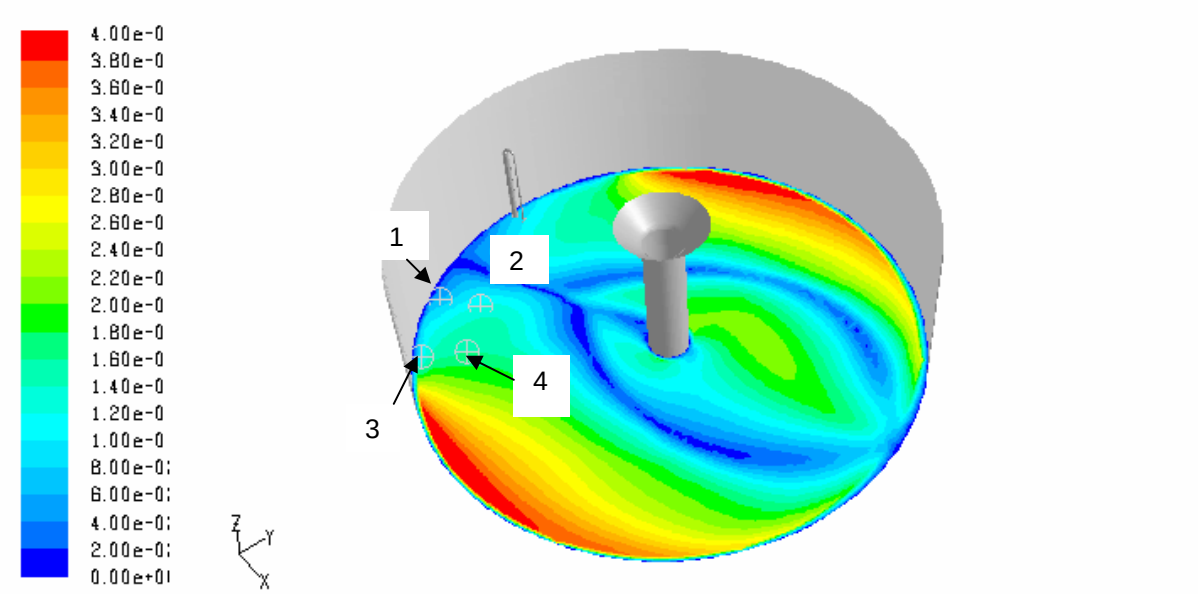

Figure 14. Velocity flow patterns and local velocity measurement locations at 2 in elevation for the Case 1 modeling conditions

Table 7. Quantitative comparison of the modeling predictions to the test results for the local positions near the tank bottom (Measurement positions of local velocities for $U_o d_o$ = 0.81 ft^2/sec.

Positions (inches)	CFD results (Case 1) (ft/sec)	Test results (ft/sec)	
Elevation/Dist. from wall (Azimuthal angle from pump)		Avg. value	Uncertainty
2 / 2 (20°)	0.073	0.1690	0.2430
2 / 10 (20°)	0.113	0.0040	0.2300
2 / 2 (40°)	0.126	0.159	0.397
2 / 10 (40°)	0.170	0.052	0.259
2 / 2 (60°)	0.439	0.511	0.305
2 / 10 (60°)	0.199	0.2010	0.3540
2 / 2 (80°)	0.416	0.5620	0.2420
2 / 10 (80°)	0.307	0.3400	0.4190
4 / 10 (60°)	0.075	0.0370	0.2360
2 / 10 (40°)	0.038	0.1060	0.2010
4 / 2 (60°)	0.038	0.2010	0.3020
4 / 2 (40°)	0.010	0.0150	0.1880
8 / 2 (40°)	0.069	0.0390	0.2390
8 / 2 (60°)	0.017	0.1050	0.2920
8 / 10 (40°)	0.082	0.0170	0.1930
8 / 10 (60°)	0.036	0.0620	0.2140

Table 8. Quantitative comparison of the modeling predictions to the test results for the local positions near the tank bottom ($U_o d_o$ = 0.83 ft^2/sec, Case 2).

Positions (inches)	CFD results (Case-2) (ft/sec)	Test results (ft/sec)	
Elevation/Dist. from wall (Azimuthal angle from pump)		Avg. value	Uncertainty
2 / 2 (20^o)	0.142	0.044	0.182
2 / 10 (20^o)	0.204	0.034	0.256
2 / 10 (40^o)	0.142	0.206	0.214
2 / 2 (40^o)	0.105	0.154	0.18
2 / 10 (60^o)	0.108	0.325	0.224
2 / 2 (60^o)	0.117	0.563	0.225
2 / 10 (80^o)	0.106	0.420	0.282
2 / 2 (80^o)	0.209	0.557	0.215
4 / 2 (60^o)	0.348	0.452	0.244
4 / 10 (60^o)	0.120	0.060	0.188
4 / 2 (40^o)	0.029	0.017	0.178
4 / 10 (40^o)	0.094	0.117	0.181
8 / 2 (40^o)	0.091	0.063	0.2
8 / 10 (40^o)	0.054	0.138	0.181
8 / 2 (60^o)	0.076	0.408	0.301
8 / 10 (60^o)	0.089	0.082	0.185

Table 9. Quantitative comparison of the modeling predictions to the test results for the local positions near the tank bottom ($U_o d_o$ = 0.81 ft^2/sec, Case2.

Positions (inches)	CFD results (Case-2) (ft/sec)	Test results (ft/sec)		Comments
Elevation/Dist. from wall (Azimuthal angle from pump)		Avg. value	Uncertainty	
2 / 2 (20^o)	0.142	0.194	0.117	
2 / 2 (40^o)	0.105	0.173	0.238	
2 / 2 (60^o)	0.117	0.445	0.25	
2 / 2 (80^o)	0.209	0.417	0.249	
2 / 10 (20^o)	0.204	0.092	0.203	
2 / 10 (40^o)	0.142	0.165	0.238	
2 / 10 (60^o)	0.108	0.303	0.279	
2 / 10 (80^o)	0.106	0.334	0.32	
8 / 10 (80^o)	0.121	0.137	0.277	
8 / 10 (60^o)	0.089	0.170	0.247	
8 / 13.5 (40^o)	0.044	0.046	0.304	
2 / 13.5 (20^o)	0.044	0.091	0.239	
2 / 13.5 (40^o)	0.244	0.122	0.250	
2 / 13.5 (80^o)	0.089	0.240	0.326	
16 / 2 (40^o)	0.886	0.536	1.882	
16/ 2 (40^o)	0.886	1.142	0.541	

Table 10. Quantitative comparison of the modeling predictions to the test results for the local positions near the tank bottom ($U_o d_o$ = 0.58 ft^2/sec).

Positions (inches)	CFD results (Case-11a) (ft/sec)	Test results (ft/sec)		Comments
Elevation/Dist. from wall (Azimuthal angle from pump)		Avg. value	Uncertainty	
2 / 2 (40°)	0.082	0.090	0.083	
2 / 10 (40°)	0.109	0.076	0.132	
2 / 2 (60°)	0.116	0.139	0.114	
2 / 2 (60°)	0.038	0.083	113.0	Axial velocity
2 / 2 (80°)	0.077	0.174	0.111	
2 / 10 (60°)	0.173	0.149	0.124	
2 / 10 (80°)	0.138	0.160	0.125	
2 / 2 (20°)	0.004	0.032	0.131	
2 / 2 (20°)	0.001	0.073	0.111	Axial velocity
2 / 10 (20°)	0.014	0.046	0.151	
4 / 2 (40°)	0.045	0.088	0.081	
4 / 2 (40°)	0.115	0.118	0.092	Axial velocity
4 / 10 (40°)	0.051	0.041	0.105	
4 / 2 (60°)	0.035	0.112	0.147	
4 / 2 (60°)	0.182	0.173	0.142	Axial velocity
4 / 10 (60°)	0.066	0.049	0.111	
8 / 2 (40°)	0.001	0.045	0.096	
8/ 2 (40°)	0.129	0.035	0.143	Axial velocity
8 / 10 (40°)	0.035	0.043	0.143	
8 / 2 (60°)	0.009	0.102	0.158	
8 / 2 (60°)	0.209	0.148	0.137	Axial velocity
8 / 10 (60°)	0.009	0.058	0.128	

Table 11. Quantitative comparison of the modeling predictions to the test results for the local positions near the tank bottom ($U_o d_o$ = 0.58 ft^2/sec).

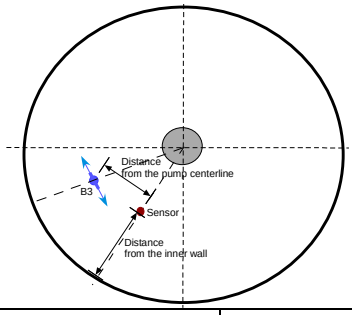

Positions (inches)	CFD results (Case-11b) (ft/sec)	Test results	
Elevation/Dist. from wall (Dist. from pump centerline)		Avg. vel. (ft/sec)	Uncertainty
16.0625 / 9.75 (20.25)	0.103	0.254	0.39
16.0625 / 11.75 (16)	0.121	0.361	0.62
16.0625 / 13.25 (12)	0.143	0.569	1.55
18.0625 / 13.25 (12)	1.682	2.651	0.36
19.0625 / 13.25 (12)	1.521	2.052	0.42
17.0625 / 13.25 (12)	0.764	1.000	0.50
18.0625 / 12.5 (14)	1.270	1.422	0.83
19.0625 / 12.5 (14)	1.388	2.312	0.38
20.0625 / 12.5 (14)	1.172	0.523	0.39
22.0625 / 11.5 (16)	0.711	0.979	0.68
21.0625 / 11.5 (16)	0.986	0.780	0.51
22.0625 / 11.5 (16)	0.711	0.435	0.47
23.0625 / 11.5 (16)	0.467	0.261	0.32
18.0625 / 11.5 (16)	1.031	0.473	0.45
16.0625 / 12.5 (14)	0.132	0.272	0.66
17.0625 / 13.75 (12)	0.817	0.698	0.86
16.0625 / 13.75 (12)	0.148	0.263	0.32
18.0625 / 13.75 (12)	1.636	1.489	

Table 12. Quantitative comparison of the modeling predictions to the test results for the local positions near the tank bottom ($U_o d_o$ = 0.70 ft^2/sec).

Positions (inches)	CFD results (Case-12a) (ft/sec)	Test results (ft/sec)	
Elevation/Dist. from wall (Azimuthal angle from pump)		Avg. value	Uncertainty
2 / 10 (20°)	0.011	0.038	0.044
2 / 2 (40°)	0.055	0.058	0.051
2 / 4 (40°)	0.081	0.031	0.052
2 / 10 (40°)	0.087	0.044	0.040
2 / 10 (40°)	0.087	0.044	0.040
4 / 10 (40°)	0.029	0.016	0.049
8 / 10 (40°)	0.030	0.032	0.075
2 / 10 (60°)	0.101	0.082	0.058
4 / 10 (60°)	0.021	0.033	0.061
2 / 10 (80°)	0.106	0.101	0.077
2 / 2 (60°)	0.012	0.098	0.096
2 / 2 (60°)	0.098	0.103	0.079
2 / 2 (60°)	0.098	0.103	0.079
4 / 2 (60°)	0.027	0.044	0.087
8 / 2 (60°)	0.012	0.098	0.096
2 / 2 (80°)	0.080	0.152	0.074
2 / 2 (60°)	0.098	0.084	0.093

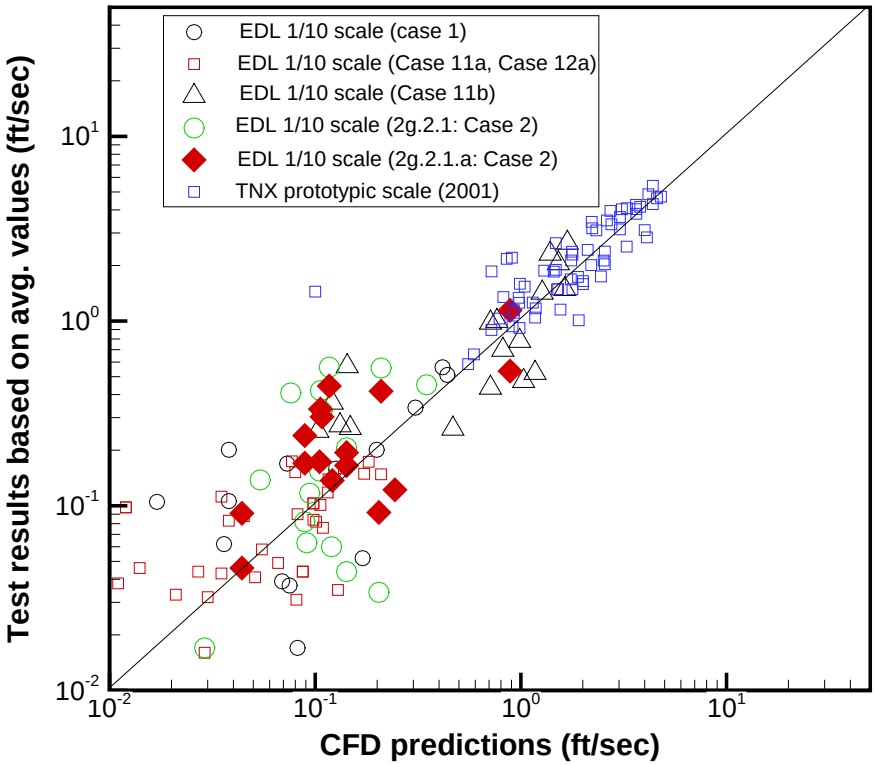

Figure 15. Benchmarking results of CFD predictions against the EDL and TNX test results for local velocities inside the EDL-scale tank with and without cooling coils (EDL cases: Case 1, Case 2 (2g.2.1 and 2g.2.1.a), Case 11a, 11b, and case 12a)

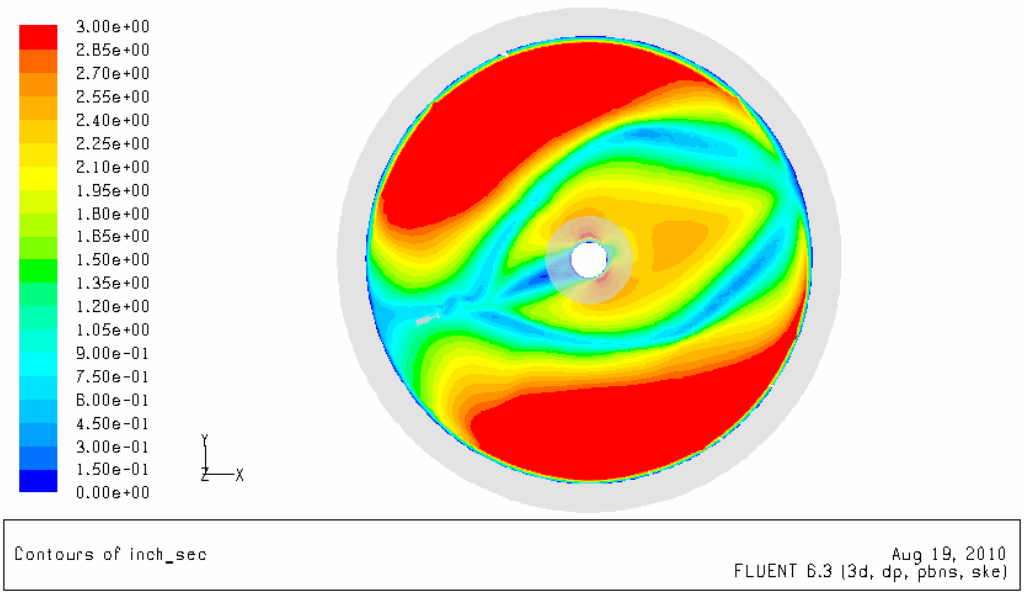

(Flow velocity at the plane 1 inch above the tank floor for the jet flow of 9.95 gpm ($U_o d_o$ = 0.81 ft^2/sec: Case 1))

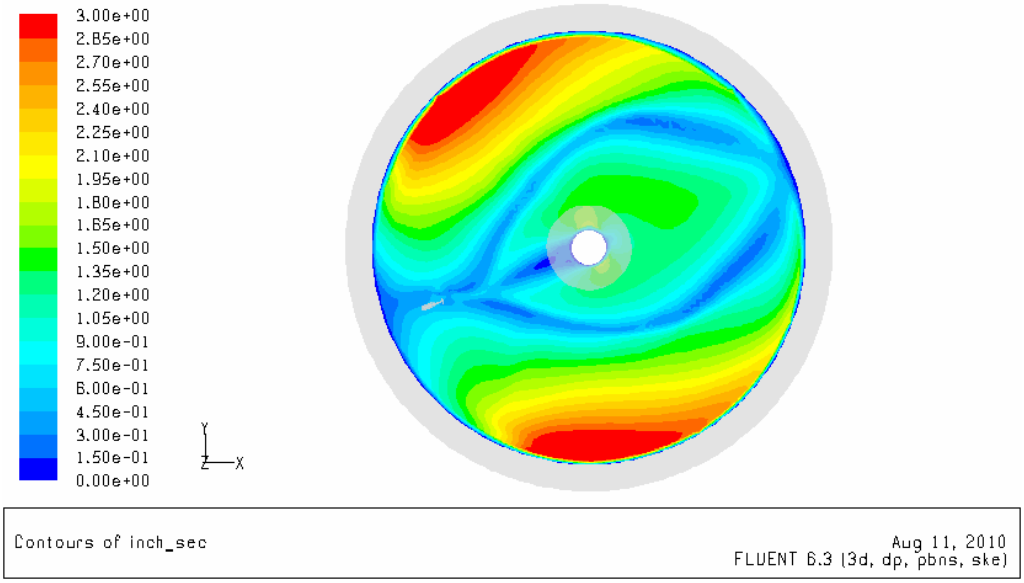

(Flow velocity at the plane 1 inch above the tank floor for the jet flow of 5.77 gpm ($U_o d_o$ = 0.47 ft^2/sec: Case 5)

Figure 16. Comparison of flow velocity distributions at the plane 1 inch above the tank floor between two typical jet flow rates of 10 and 6 gpm for the EDL tank with no cooling coils

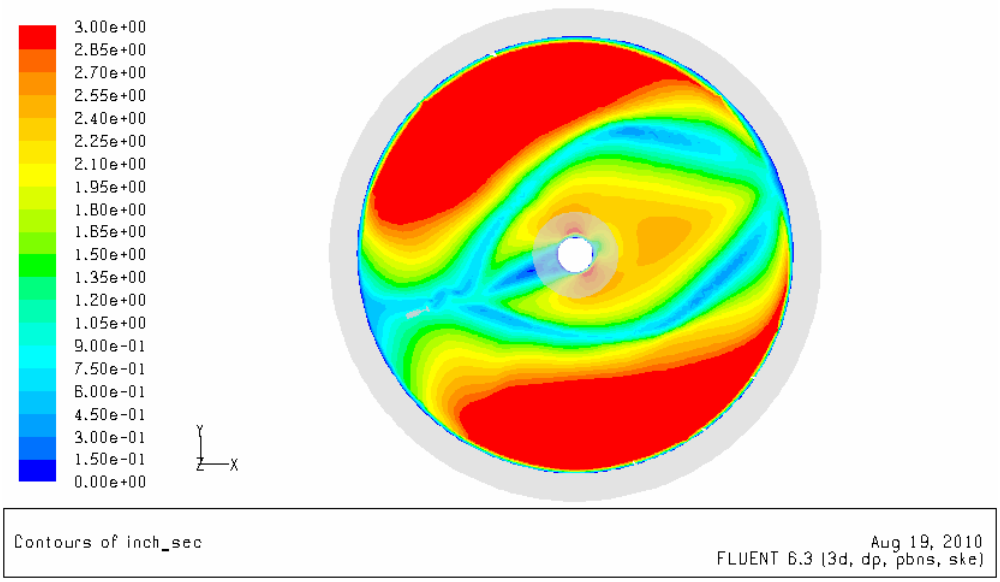

(Case 1: Flow velocity with no cooling coils)

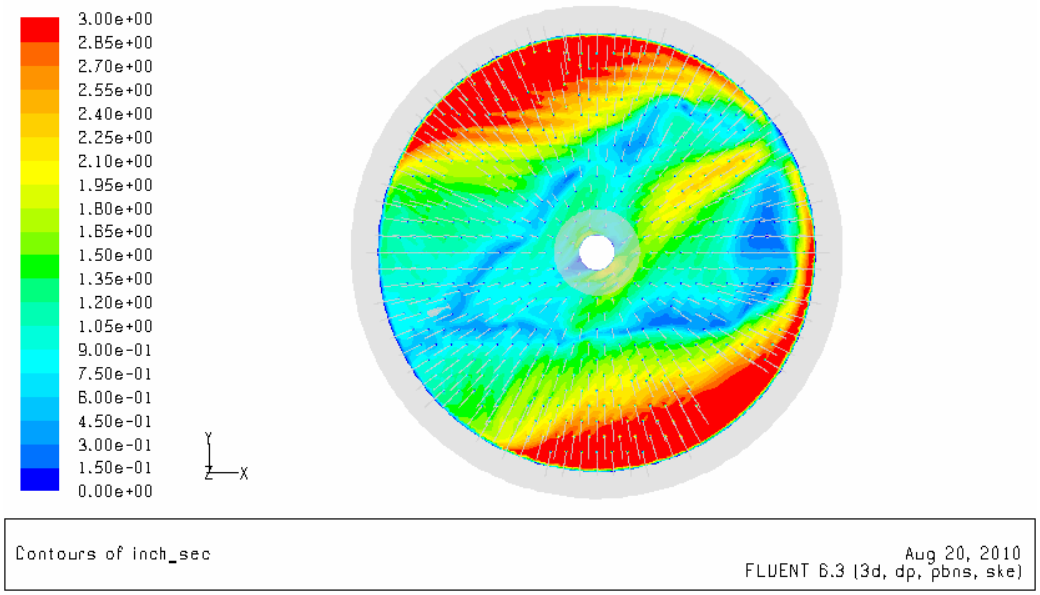

(Case 3: Flow velocity with cooling coils)

Figure 17. Comparison of flow velocity distributions at the plane 1 inch above the tank floor for the EDL tank without and with cooling coils for 9.95 gpm, $U_o d_o$ = 0.81 ft^2/sec under the same color map

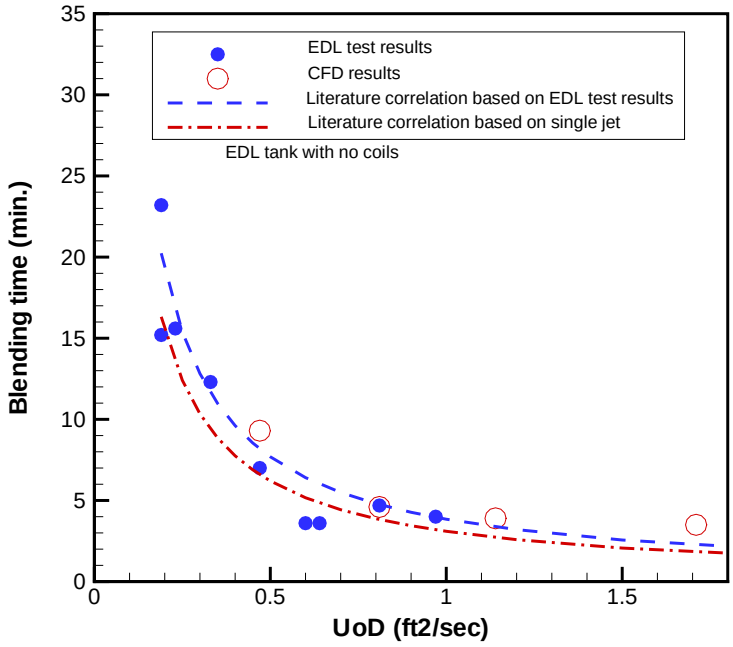

Figure 18. Benchmarking results of EDL tank with no coils against the EDL test results for the water-acid blending time

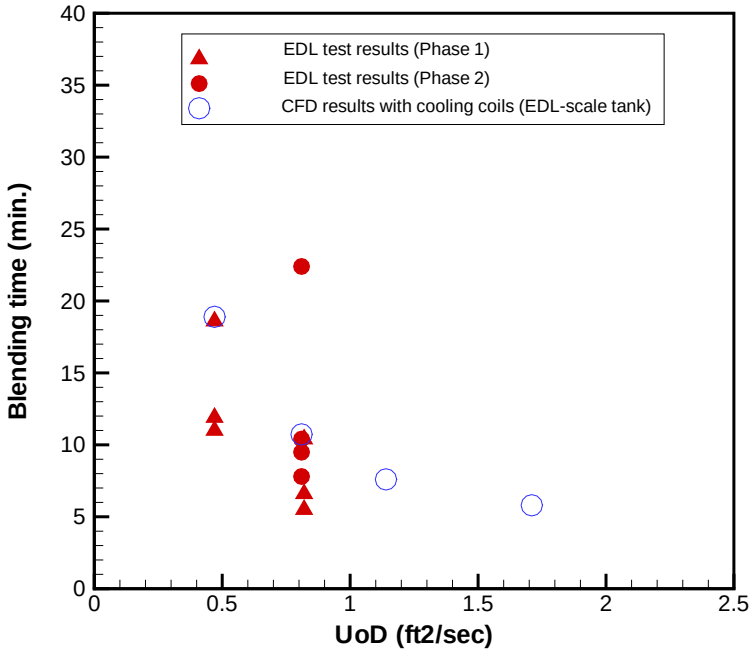

Figure 19. Benchmarking results of EDL tank with coils against the EDL test results for the water-acid blending time

5.2 Performance Modeling Results

The CFD modeling predictions for the jetted mainstream velocities along the principal discharge direction of the blending pump, and local velocities for the remote boundary regions near the sludge layer were benchmarked against the test results. Based on the validated CFD model, the current work consists of two main goals. One goal is to identify a suitable pumping $U_o d_o$ value that will adequately blend two miscible liquids to obtain a uniform composition in the tank with a minimum level of sludge solid particulate in suspension. In this case, the blending time for the suitable pump design was estimated by using the CFD models for Tank 50H without and with cooling coils. The other is to estimate the elevation in the tank at which the transfer pump inlet should be located where the solid concentration of the entrained fluid remains at a minimum level during transfer operation to the Salt Waste Processing Facility.

A series of performance calculations were performed to determine an optimum $U_o d_o$ value of dual jet pump. All cases modeled for the analysis are summarized in Table 2. For the performance analysis, the modeling calculations were based on the 15^o upward V-shape pump since the V-shape pump was identified by the phase-II experimental study to investigate the limited disturbance of the sludge layer. As observed by the EDL experimental study, top surface of the thin sludge layer settled on the tank floor was not disturbed at all under 0.47 ft^2/sec pump operation. Figure 20 shows velocity distributions at the top surface of the sludge layer for the EDL tank with no cooling coils (Case 10). The results show that the maximum speed is about 0.28 ft/sec at both sides of the pump located at parallel to the tank wall.

When the $U_o d_o$ value of the upward V-shape pump submerged in nitrate solution is 0.58 ft^2/sec for Case 11a, local velocities are shown in Fig. 21. The experimental results for Case 11a show that no solids were scoured from the sludge layer into the liquid zone, but the minimal level of the sludge disturbance was observed. The modeling results for the 0.58 ft^2/sec pump show that maximum velocity at the top surface of the sludge layer is 0.36 ft/sec. When the same pump is operated in nitrite solution instead of nitrate under Case 11b, similar results are shown in Fig. 22. For the CFD calculations, the top surface of the sludge layer was modeled to be frictionless, but the sludge layer was not included in the computational domain. As discussed earlier, the impact of the cooling coils on local flow velocities was not negligible for the small-scale EDL tank. Case 12b modeled the presence of cooling coils for the EDL-scale tank with 15^o V-shape operated at pump 0.7 ft^2/sec in nitrite solution. The modeling results are shown in Fig. 23. The results show that although the pumping power is increased by 17% (from 0.58 to 0.70 ft^2/sec) for the blending operation with cooling coils, local velocities for the potential impact areas are not changed significantly.

When the validated model is applied to the calculations of the steady-state flow field inside the full-scale Tank 50H with no cooling coils under the Case 13 operating conditions, velocity flow patterns at 9.49 inches above tank floor are shown in Fig. 24. The results show that maximum local velocity of the sludge surface for the 0.58 ft^2/sec EDL tank, Case 11a, is about 15% higher than that of the full scale 6.3 ft^2/sec tank, Case 13. Figure 25 shows that when the 15^0 V-shape pump with $U_o d_o$ value of 7.6 ft^2/sec is used for blending operation of the tank contents, maximum local velocity at the sludge surface is about 0.44 ft/sec.

As discussed earlier, homogeneous blending of miscible salt solutions is required before transfer of the blended solution to the SWPF. During the blending process, settled sludge is required to remain undisturbed on the bottom of waste tanks. Suspension of sludge during blending may potentially release radiolytically generated hydrogen trapped in the sludge, which is a safety concern. The transfer pump model was developed to estimate the elevation in the tank at which the transfer pump inlet should be located where the solid concentration of the entrained fluid remains at a minimum level of solids concentrations during transfer operation to the SWPF. Pilot scale experiments were performed to investigate disturbance of sludge using non-radioactive sludge simulants. As shown in Table 3, the sludge region is not included in the computational domain, and the model assumes the top surface of the sludge layer to be frictionless.

When a transfer pump is assumed to have no solid plate as an initial modeling approach (Case 15), the horizontal velocity distributions at the top surface of the sludge layer are shown in Fig. 26. The corresponding flow patterns and contour plots are presented in Figs. 27 and 28. The results show that maximum local velocity at the top surface of sludge layer is about 0.14 ft/sec. When an 1-in solid plate is placed 0.37 in below the suction inlet of transfer pump, and it is located 3/8 in above the top sludge surface as shown in Table 3 (Case 16a), maximum velocity at the sludge surface is about 0.028 ft/sec, resulting in local velocity four times lower than that of the transfer pump without the solid plate. The velocity flow patterns for the horizontal and vertical planes crossing the transfer suction inlet are shown in fig. 29. When Case 16b assumes that the 1-in solid plate of the same pump as Case 16a is placed ¼ in above the sludge surface, maximum local velocity is 0.046 ft/sec about 70% higher than that of Case 16a. The horizontal velocity distributions and vertical flow patterns are presented in Fig. 30. The modeling calculations for all three cases of Case 15, Case 16a, and Case 16b were performed for the EDL 1/10.85 scale. Figure 31 compares velocity distributions at top surface of the sludge layer for three different transfer operations in EDL scale tank. When the transfer pump has no solid plate under the pump suction inlet, maximum velocity on the top sludge surface reaches about 0.14 ft/sec, which is about three times higher than that of the pump with solid plate for the same transfer flowrate of 1.1 gpm as shown in the figure. The modeling results for the pilot scale indicate that a solid plate is very effective in reducing local velocities so that local fluid motion does not entrain the solids from the top sludge surface during the transfer operations of the blended solutions. The experimental observations made by the EDL pilot-scale test showed that no solids were entrained under the transfer pump operation of Case 16b condition. It is noted that when the pump elevation changes from 1/4 to 3/8 inches, local peak velocity is reduced by about 30%.

When the pilot scale design of the transfer pump is linearly scaled up by 10.85 times, three different cases of Case 17a to 17c are modeled in terms of the transfer inlet elevation. Maximum local velocities at the top sludge layer for three different transfer pump configurations and elevations under full-scale operations are summarized in Table 13. As shown in the table, maximum velocity at the sludge surface ranges from 0.016 ft/sec to 0.026 ft/sec depending on the elevation of the transfer pump inlet. The results are shown in Figs. 32 to 34.

The blending pump is required to mix the miscible fluid contents for preparation of salt feed batches to SWPF, and the larger pump $U_o d_o$ value provided the better blending, while the smaller pump $U_o d_o$ value minimized sludge disturbance. Modeling calculations for a range of the pump $U_o d_o$ values are required to establish adequate blending without sludge disturbance is a primary goal of the work. Thus, the blending time calculations have been

performed for a range of modeling conditions for two different pump configurations of T- and V-shape nozzles, and various flowrates of pump U_od_o values as shown in Table 2. Final performance calculations will be performed for the established CW pump design (Case 19), and the operating conditions to satisfy those two requirements of minimum sludge disturbance, and adequate blending of tank contents.

Figure 35 compares the modeling results for typical transient blending concentrations for the T-shape pump inside the EDL-scale tank with and without cooling coils under pump nozzle speed 46.5 ft/sec and U_od_o value of 0.81 ft^2/sec. The results show that the blending time for the tank with cooling coils is 10.7 minutes, while the time for the tank without cooling coils is 4.6 minutes. However, as tank volume is linearly scaled up by about 10.85 times, the blending time difference between the cases with and without cooling coils is reduced. Table 14 quantitatively compares the blending times for the EDL pilot-scale and Tank 50 full-scale tanks with T-shape pumps. Figure 36 presents impact of cooling coils on the blending time for the water-acid blending time for the EDL-scale tank. It is noted that for 1/10.85 scale tank, the blending time for the tank with coils requires about double times longer than the tank with no coils, but for full-scale tank, the blending time for the coiled case requires about 50% longer than that of the no coils case. In addition, the time difference is reduced when the pumping U_od_o value for a given EDL scale tank is increased.

Sensitivity analysis for the pump nozzle configurations has been performed to investigate the impact of the blending performance on the nozzle directions. Quantitative comparison of blending times for two different tank scales with T-shape and V-shape pumps with no coils is made in Table 15. As shown in the table, the blending time for T-shape dual jet pump is about 20% longer than that of 15^o upward V-shape pump under the EDL pilot-scale tank, while the time difference between the two pumps is about 12% for the full-scale Tank 50H. It is noticed that the impact of the pump nozzle change on the blending performance is reduced with the tank size scaled up. These results are consistent with the literature information as indicated in Summary of Sec. 3. All the modeling results for the performance analysis are summarized in Table 16.

Final performance modeling calculations has been performed by using the established CW pump design and the operating conditions to satisfy the two requirements of minimum sludge disturbance and adequate blending of tank contents. The final results for Case 19 and Case 20 are presented in Table 16. The velocity distributions at the top sludge layer settled on the tank floor are shown in Fig. 37. The results confirm that when the final CW pumps of 6.1 ft^2/sec for the coiled tank and 5.1 ft^2/sec for the uncoiled tank are used for the blending operations of miscible fluids, maximum local velocities at the top sludge surface of the full-scale coiled and uncoiled tanks are less than the velocity criterion to prevent sludge scouring, 0.36 ft/sec. It is noted that the blending time for the coiled tank with 6.1 ft^2/sec CW pump is about 2 times longer than that of the uncoiled tank with 5.1 ft^2/sec CW pump.

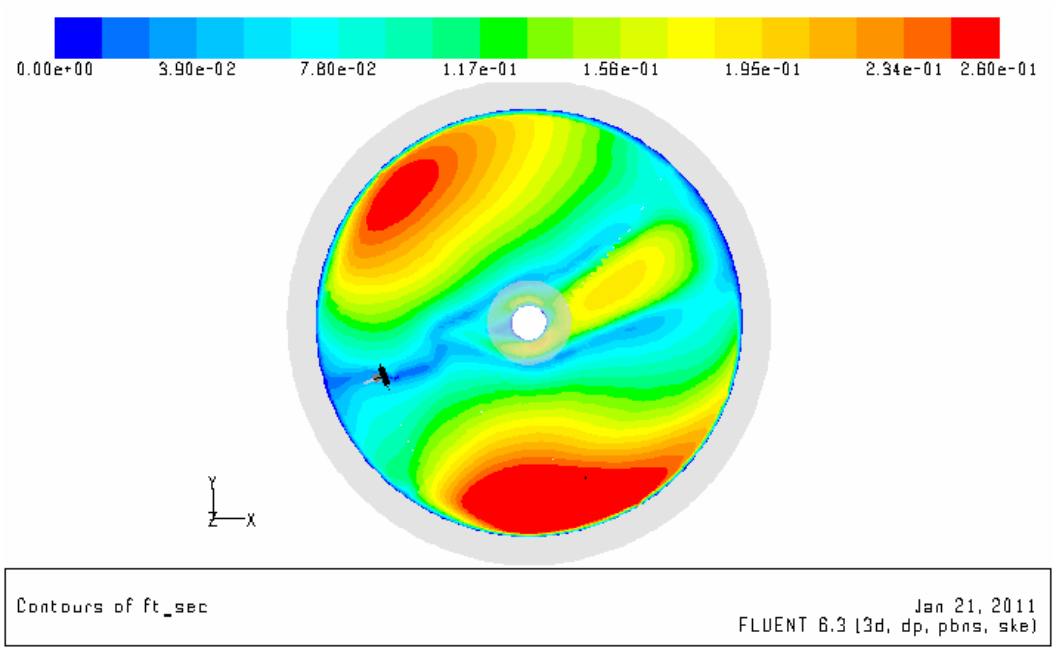

Figure 20. Velocity distributions at top surface of the sludge layer (Case 10).

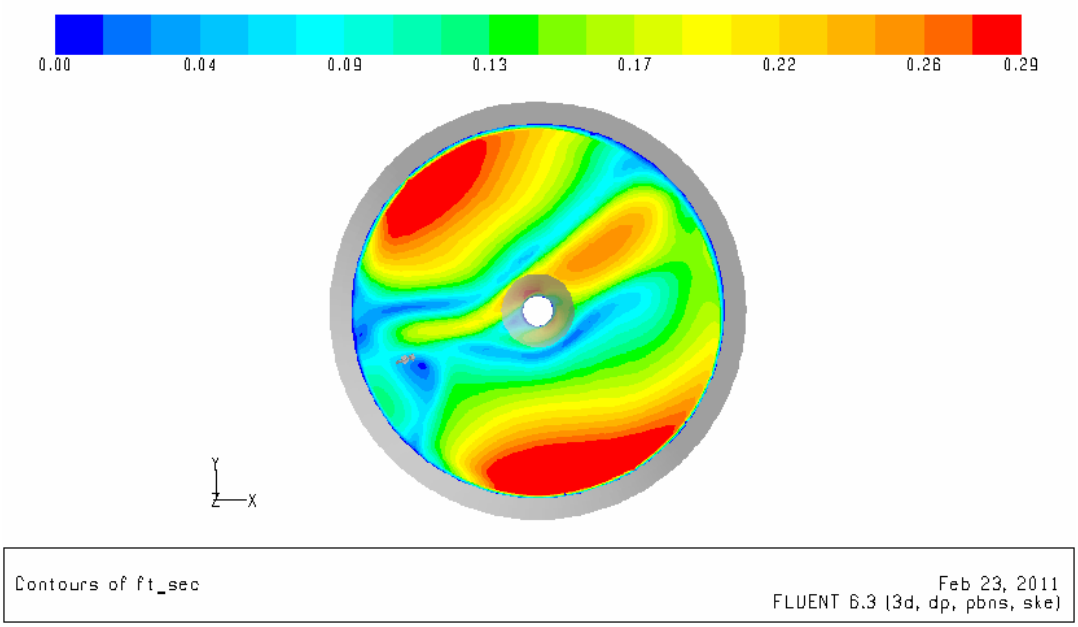

Figure 21. Velocity distributions at top surface of the sludge layer (Case 11a)

.

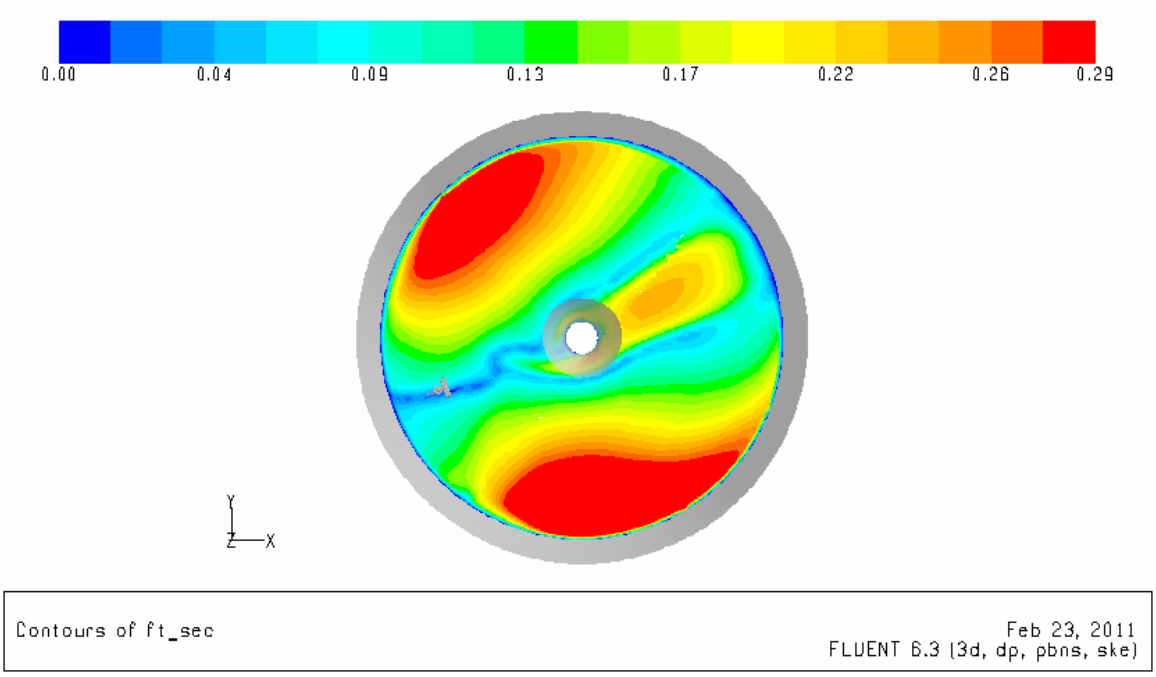

Figure 22. Velocity distributions at top surface of the sludge layer (Case 11b).

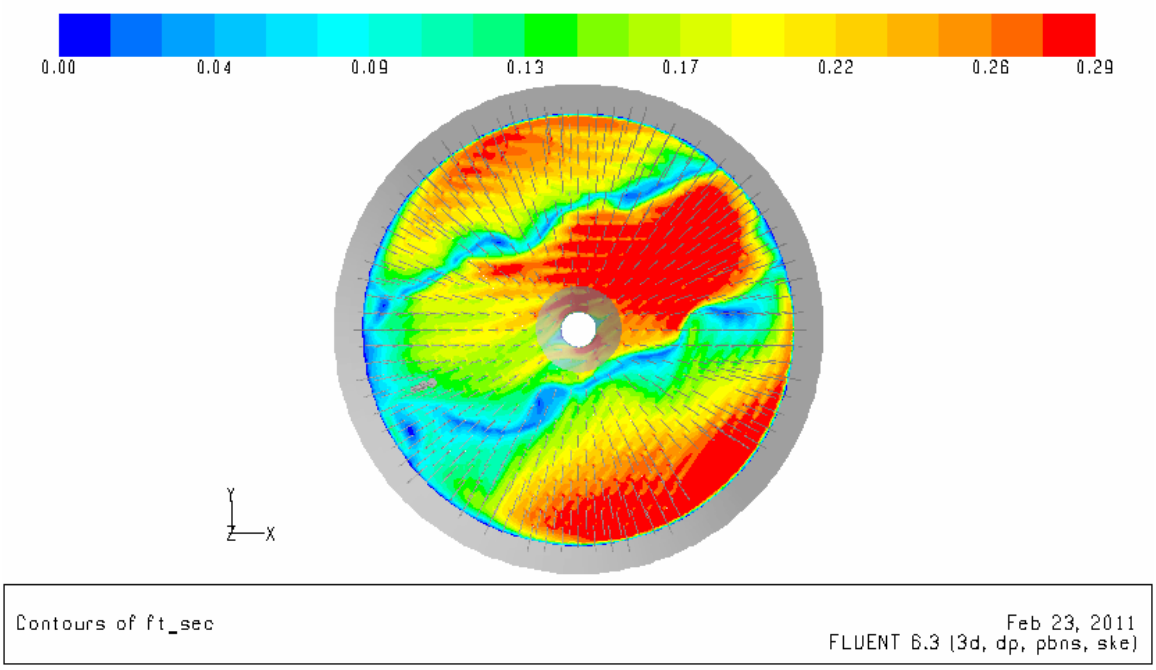

Figure 23. Velocity distributions at top surface of the sludge layer (Case 12b)

.

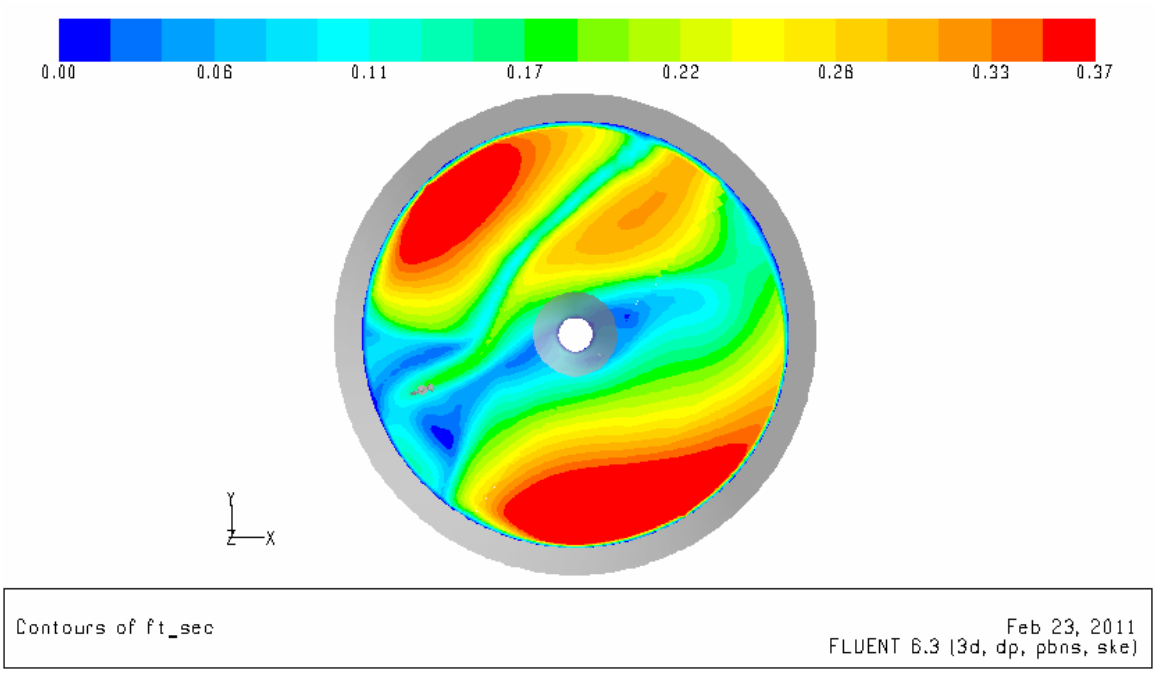

Figure 24. Velocity distributions at top surface of the sludge layer (Case 13)

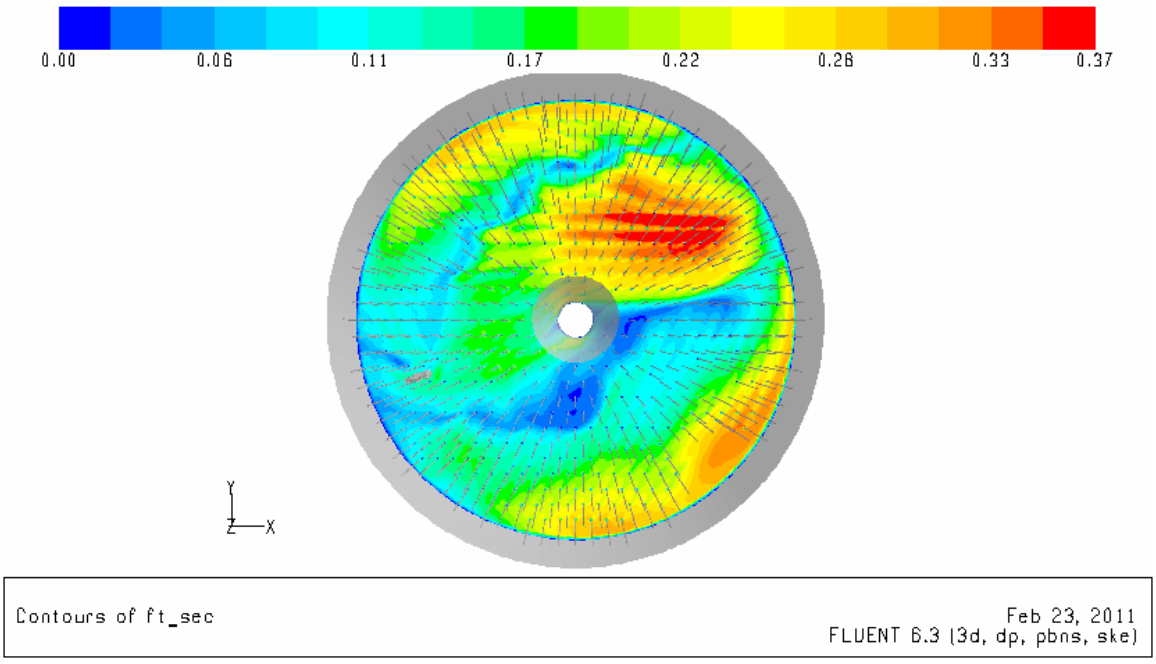

Figure 25. Velocity distributions at top surface of the sludge layer (Case 14)

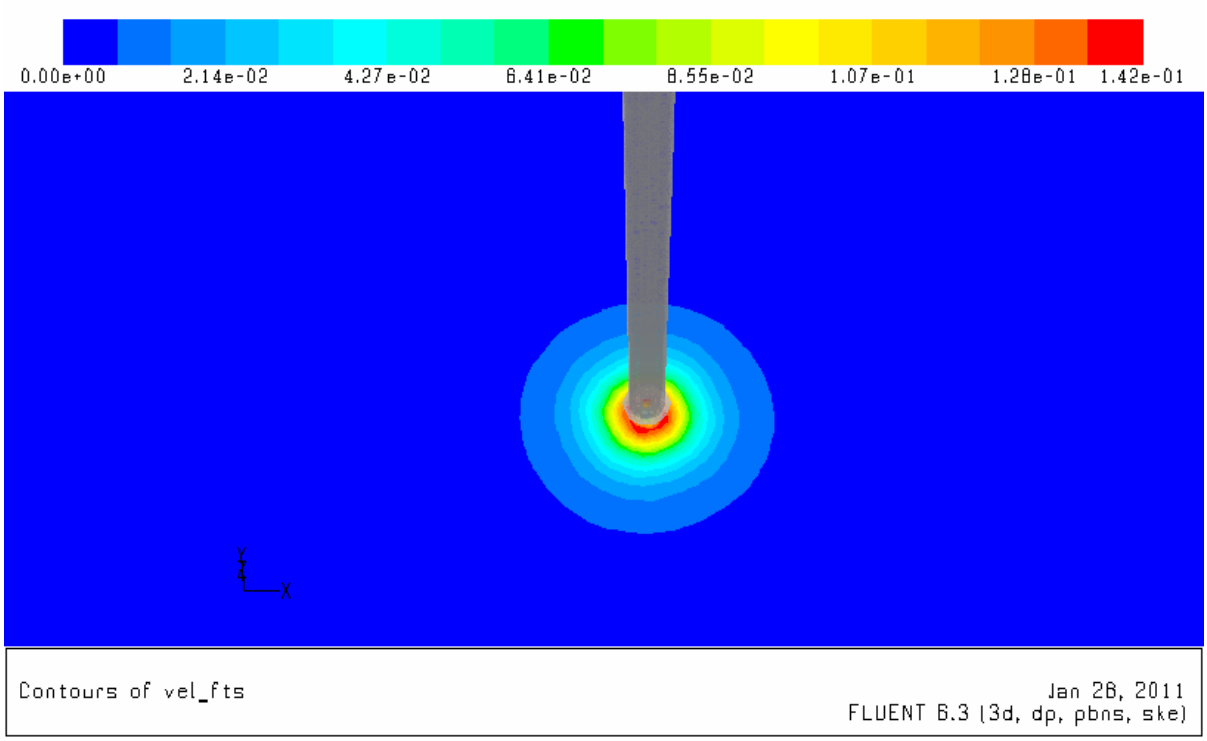

Figure 26. Velocity distributions at top surface of the sludge layer (Case 15).

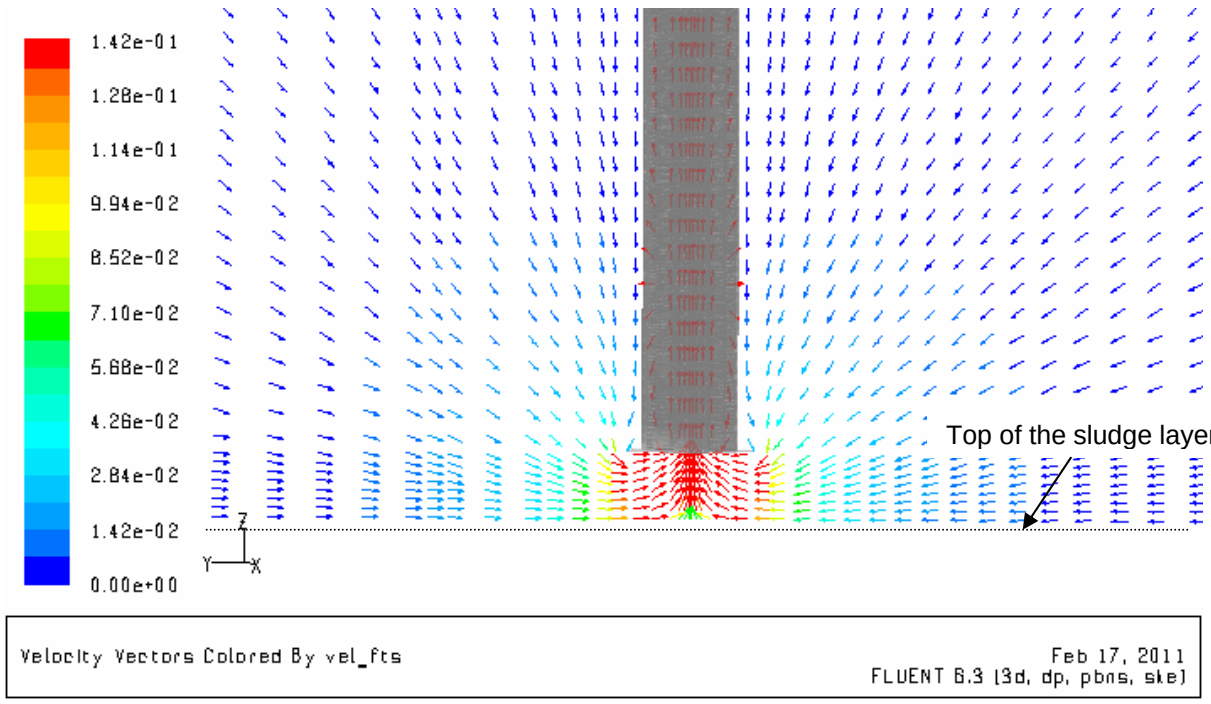

Figure 27. Velocity flow patterns at top surface of the sludge layer (Case 15).

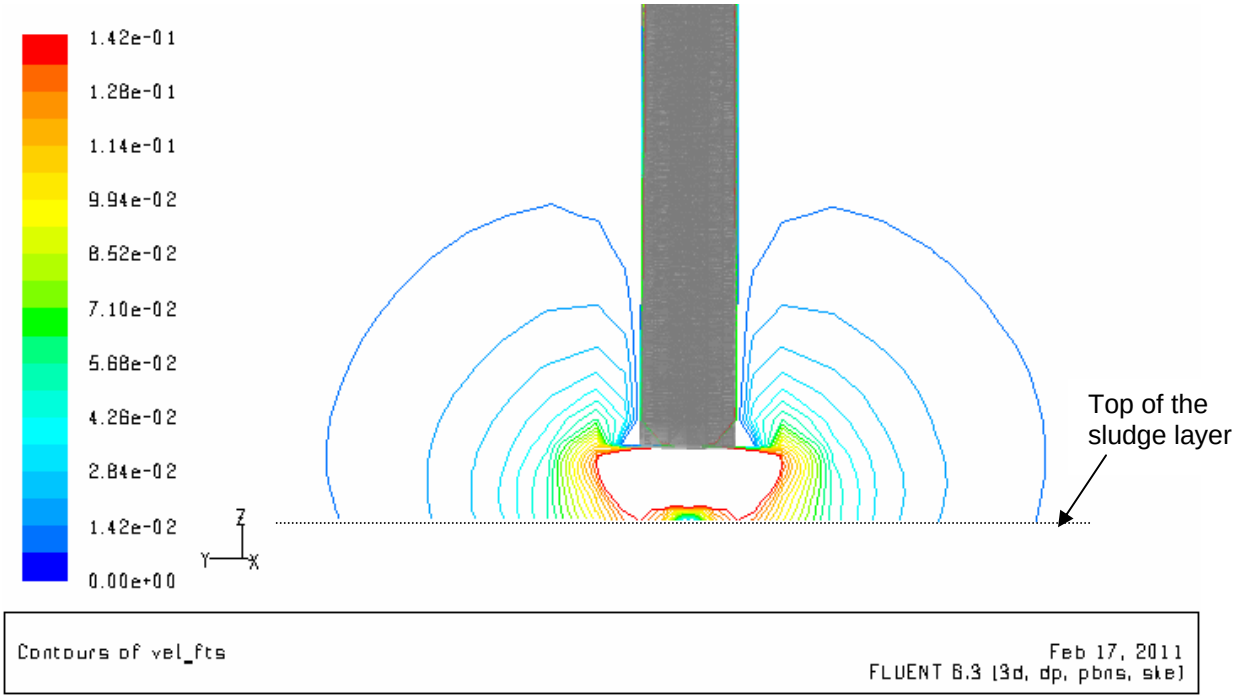

Figure 28. Velocity flow patterns at top surface of the sludge layer (Case 15).

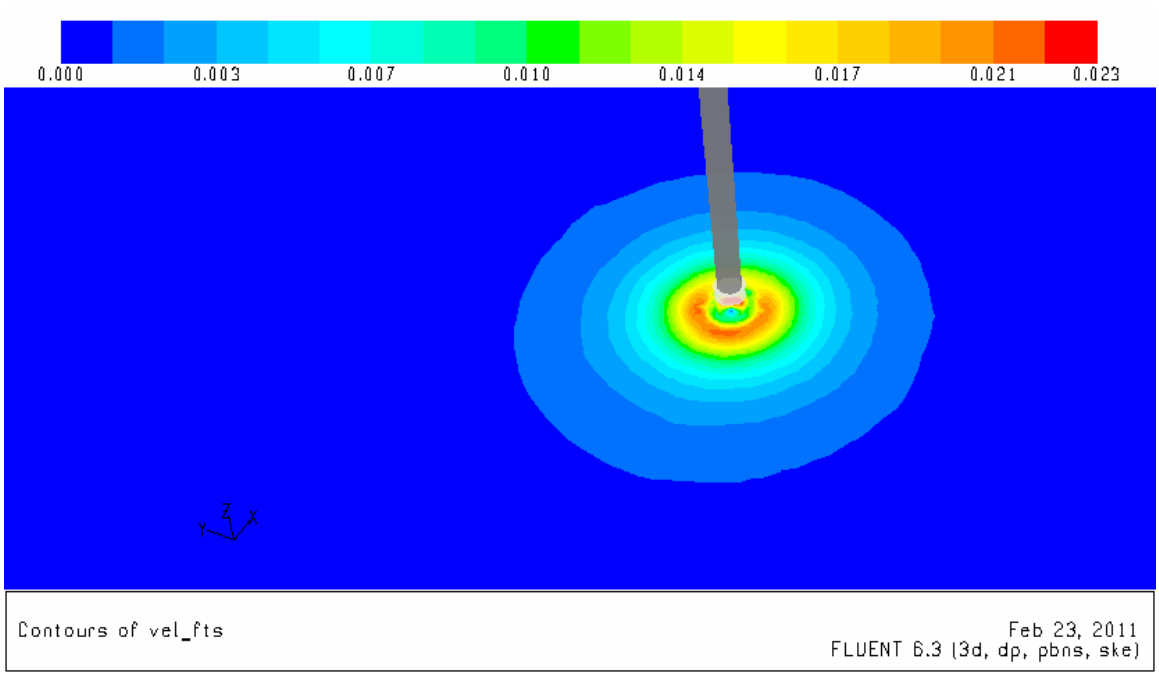

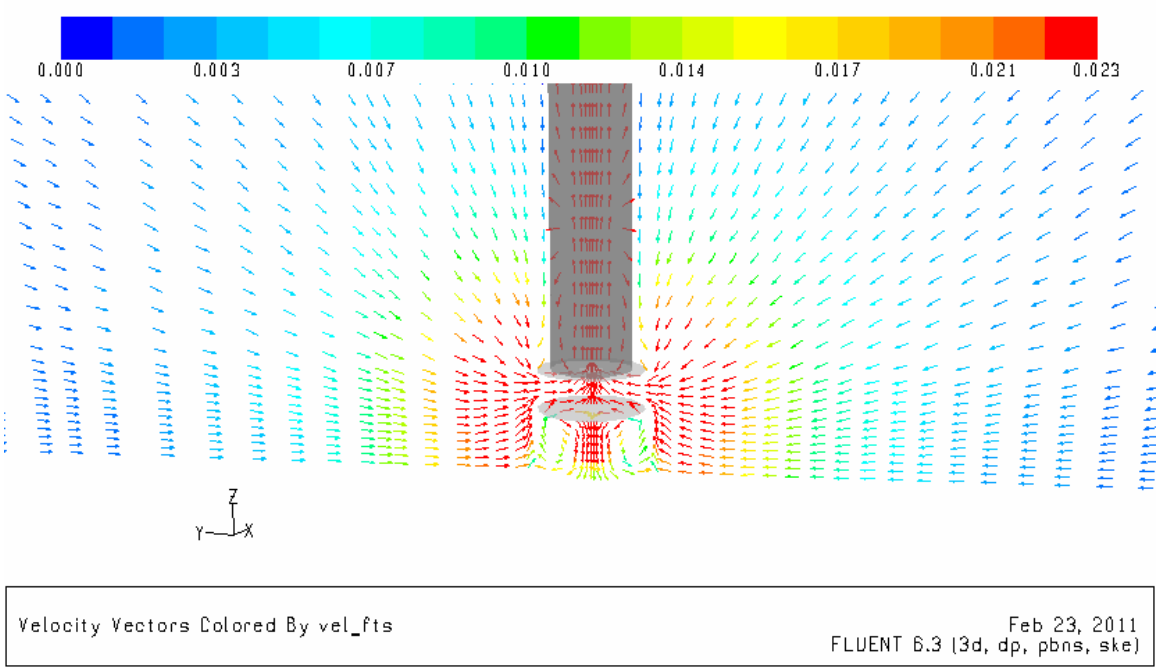

Figure 29. Velocity distributions at top surface of the sludge layer (Case 16a).

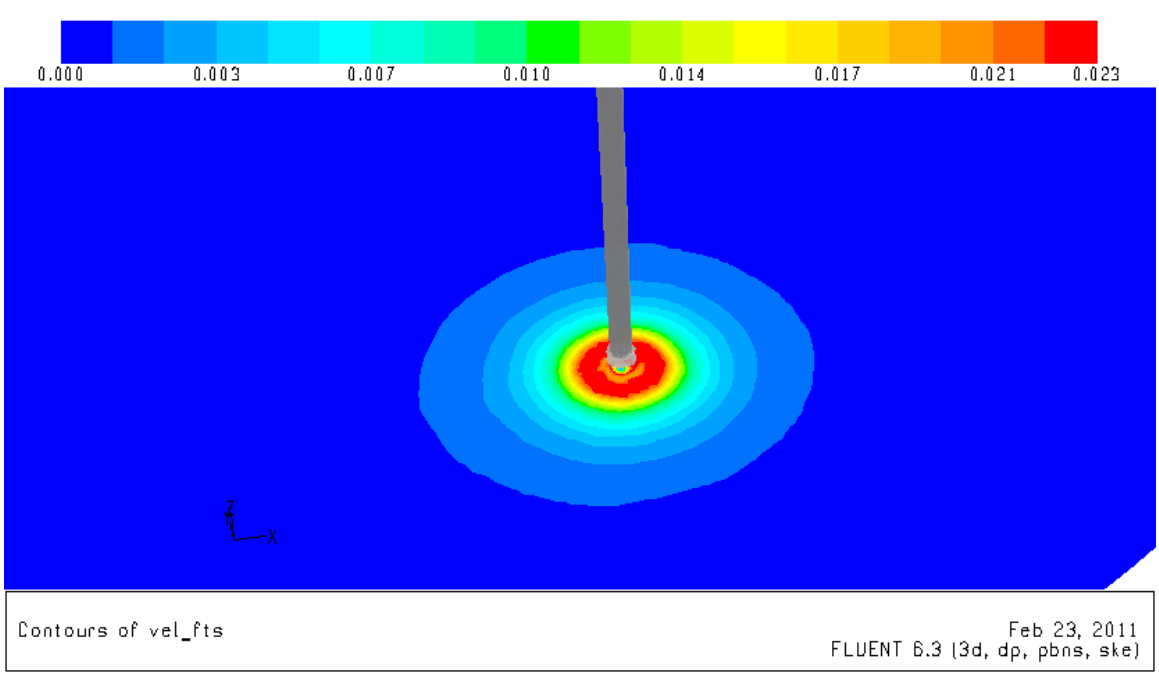

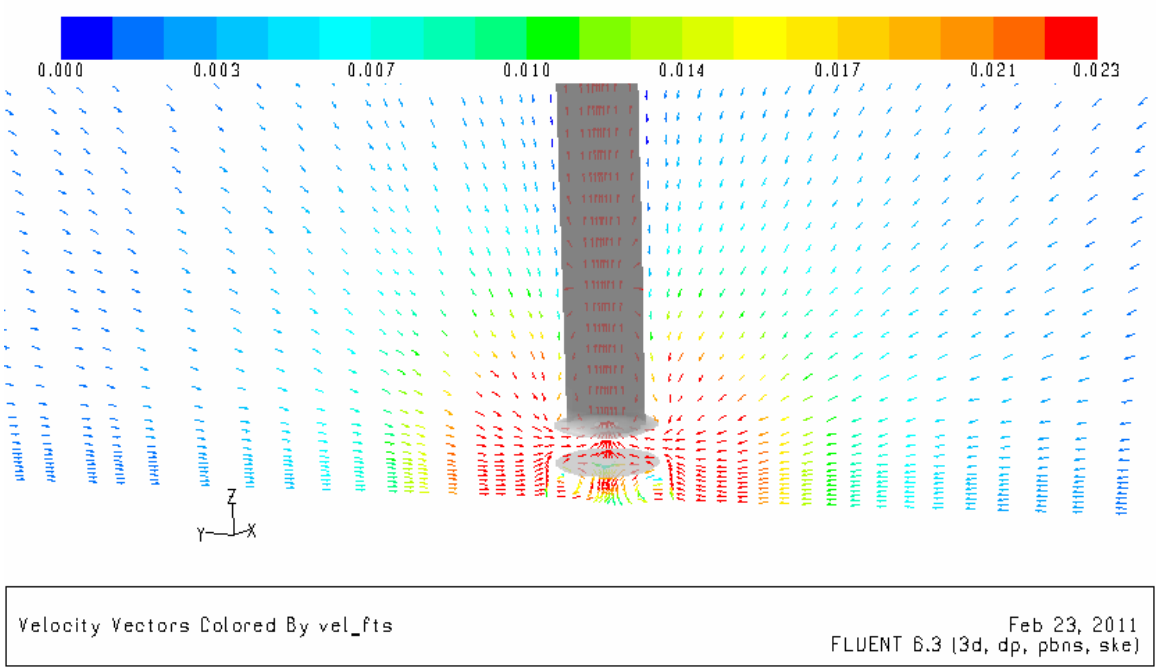

Figure 30. Velocity distributions at top surface of the sludge layer (Case 16b).

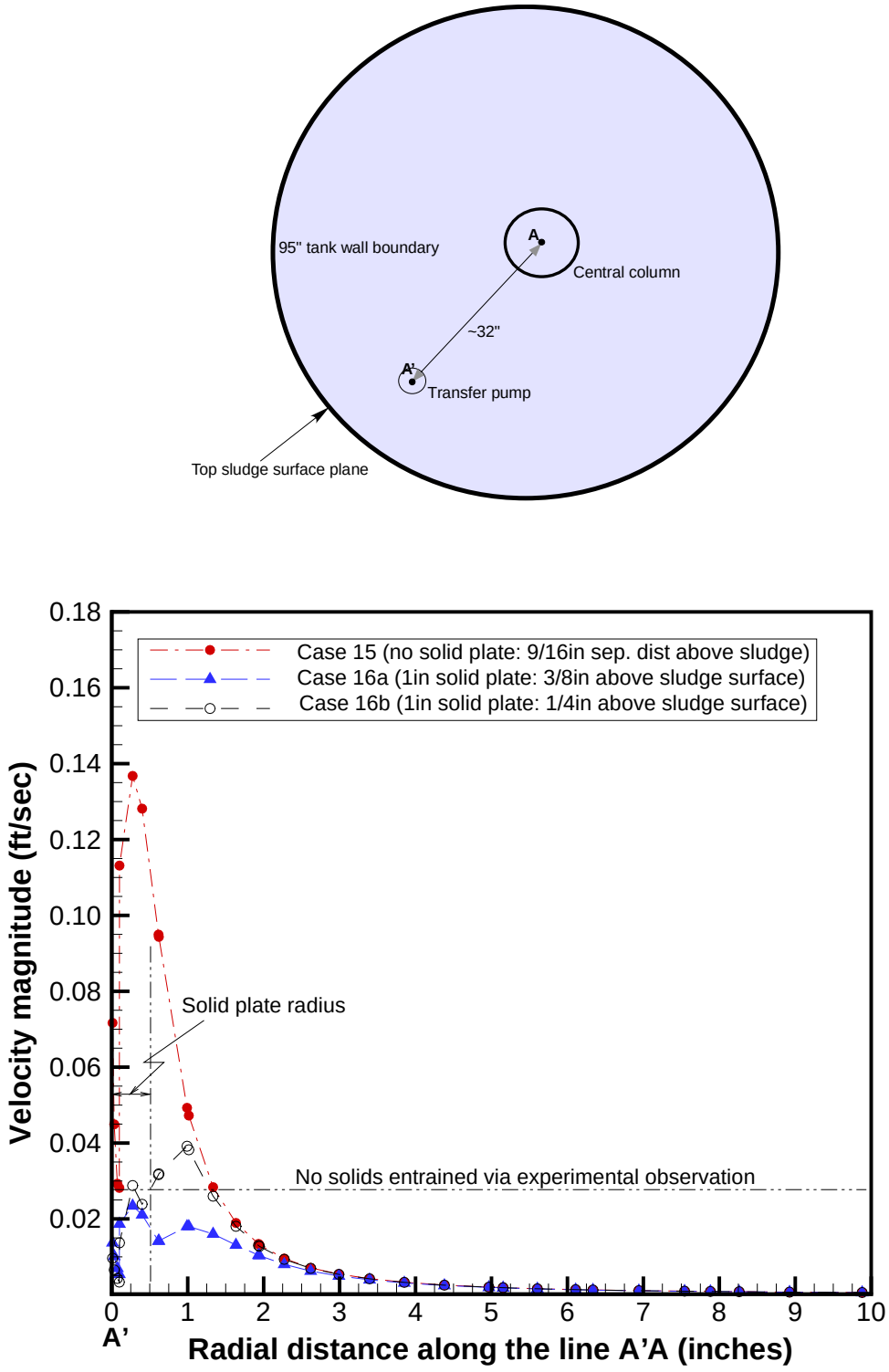

Figure 31. Velocity distributions at top surface of the sludge layer for the transfer pump operations in EDL scale tank.

Table 13. Max. local velocity at the top sludge layer for different transfer pump configurations and elevations under full-scale operations

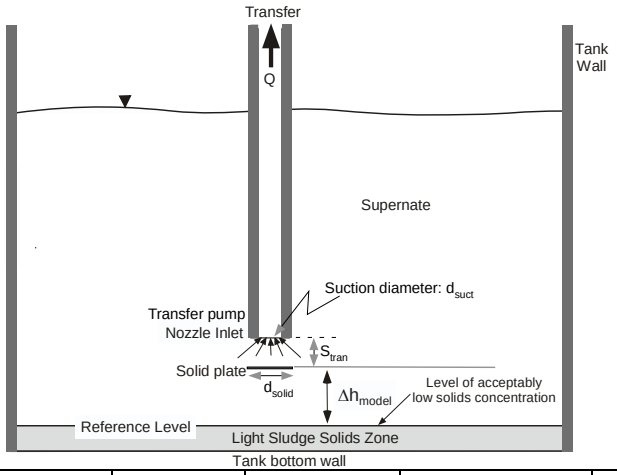

Case	Q (gpm)	d_{suct} (inches)	S_{tran} Screen height (inches)	d_{solid} (inches)	Δh_{model} (inches)	$u_{sludge,max}$ (ft/sec)
17a	130	12.5	6	18	5.43	0.021
17b	130	2.4	2	11	9.5	0.016
17c	130	2.4	4	10.85	5.43	0.026

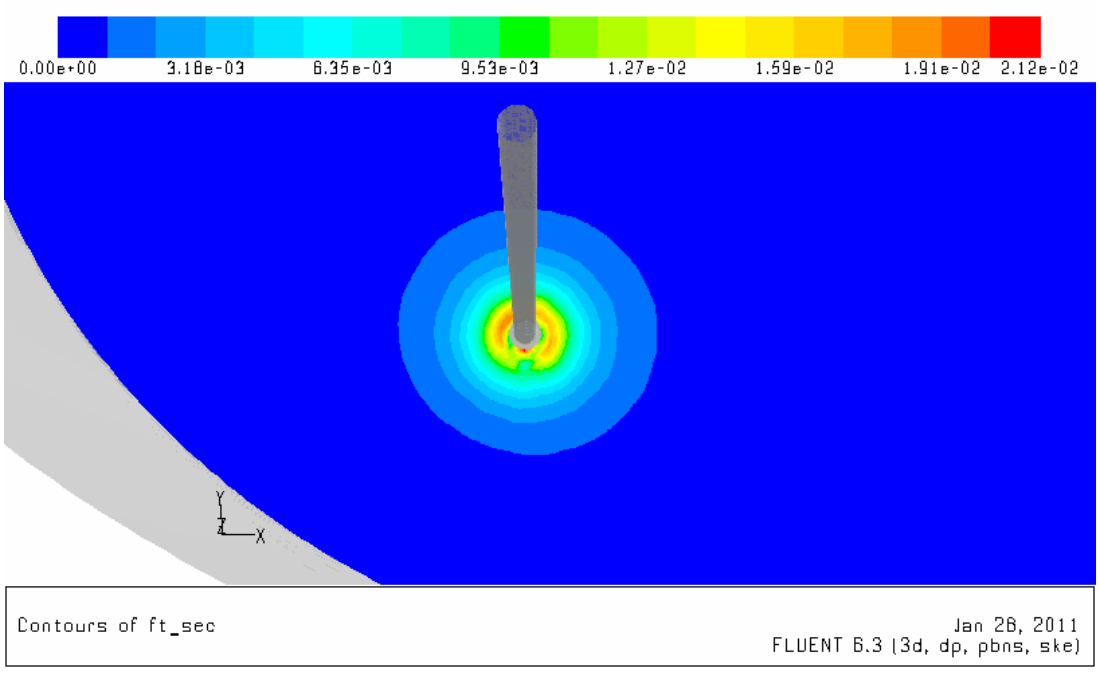

Figure 32. Velocity distributions at top surface of the sludge layer (Case 17a).

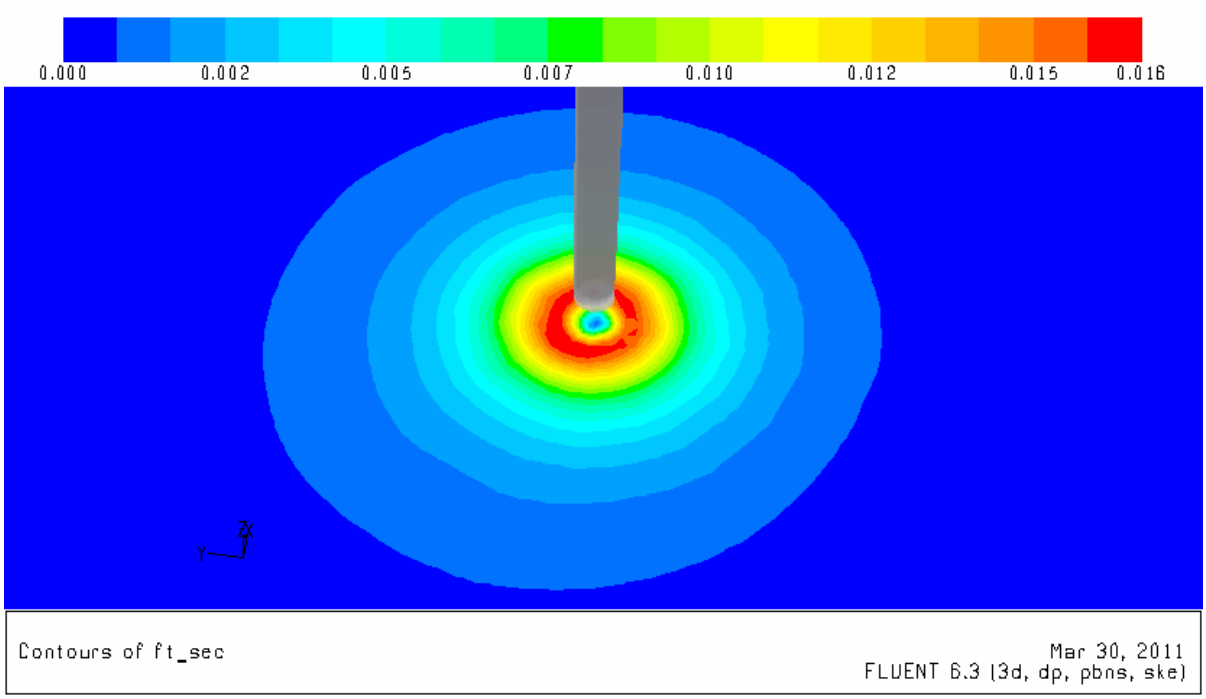

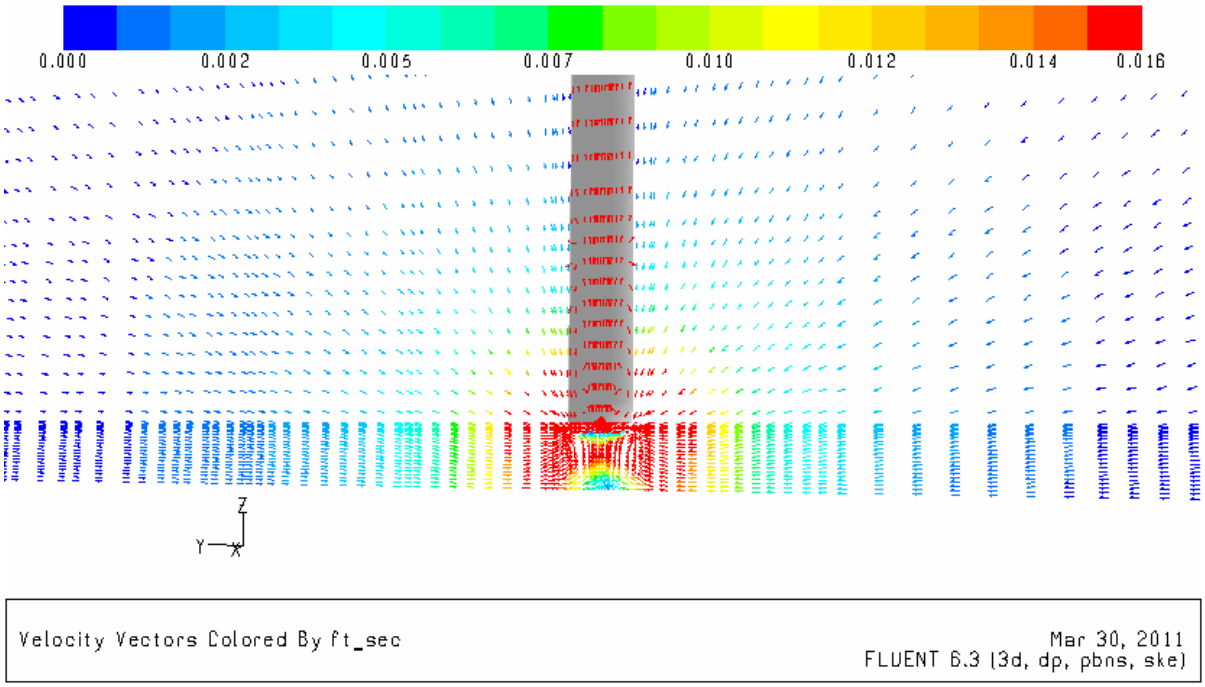

Figure 33. Velocity distributions at top surface of the sludge layer (Case 17b).

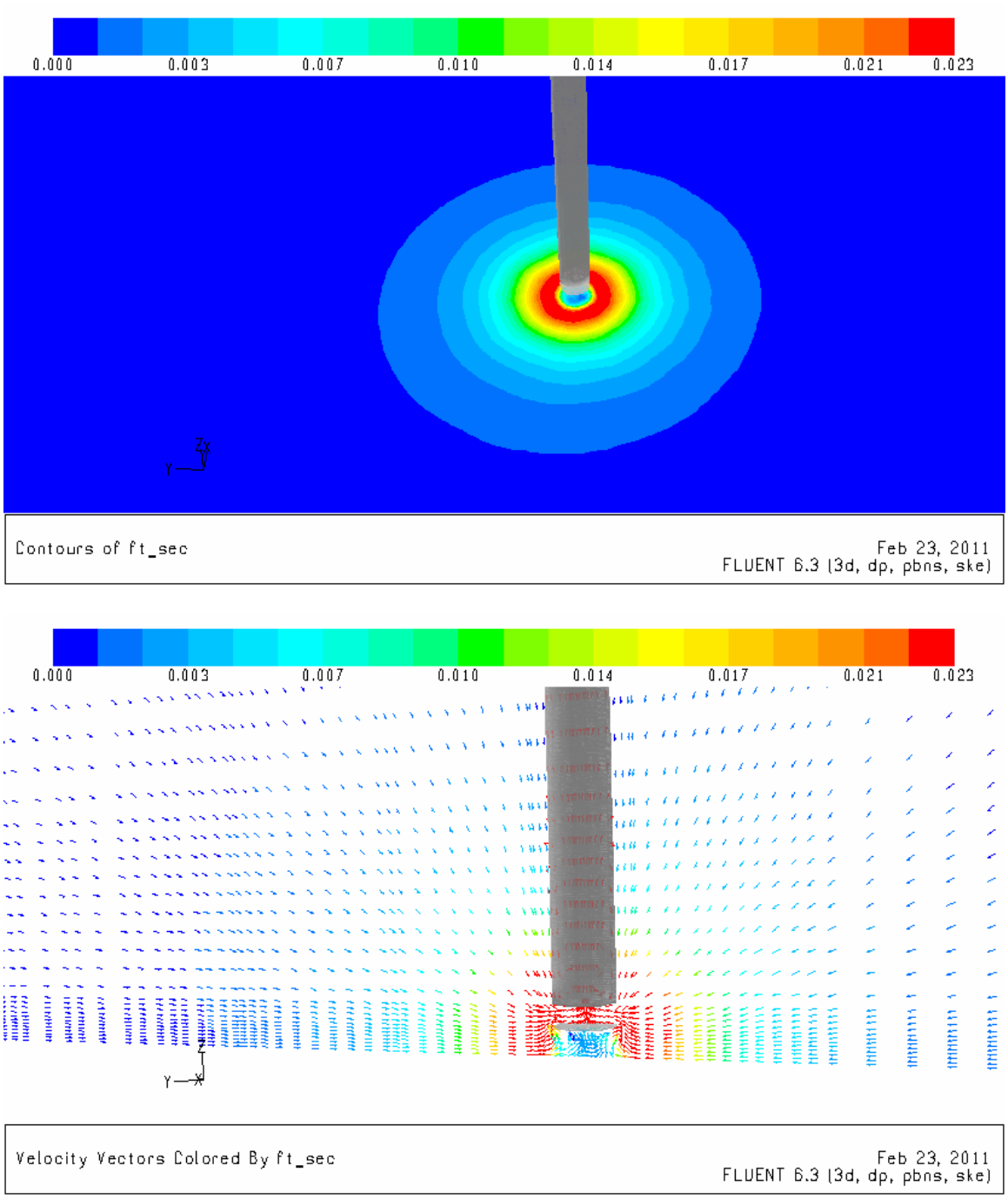

Figure 34. Velocity distributions at top surface of the sludge layer (Case 17c).

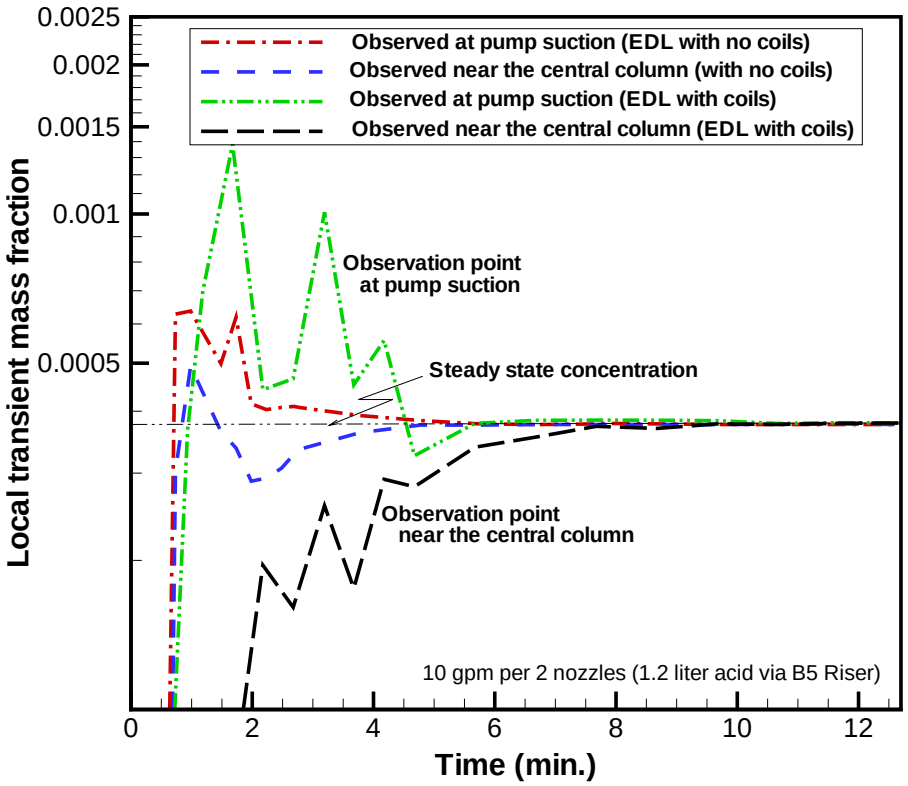

Figure 35. Comparison of transient blending concentrations for the T-shape pump inside the EDL tank with and without cooling coils (Nozzle speed = 46.5 ft/sec, $U_o d_o$ = 0.81 ft^2/sec)

Table 14. Quantitative comparison of blending times for the EDL scale-down and full-scale tanks with T-shape pumps

System scale	Coil presence inside tank	Pumping fluid-tracer	$U_o d_o$ (ft^2/sec)	Blending time (min.)
Scale down (EDL)	No	Water-acid	0.47	9.3
	Yes	Water-acid	0.47	18.9
Full scale	No	Water-acid	8.8	64.0
	Yes	Water-acid	8.8	99.5

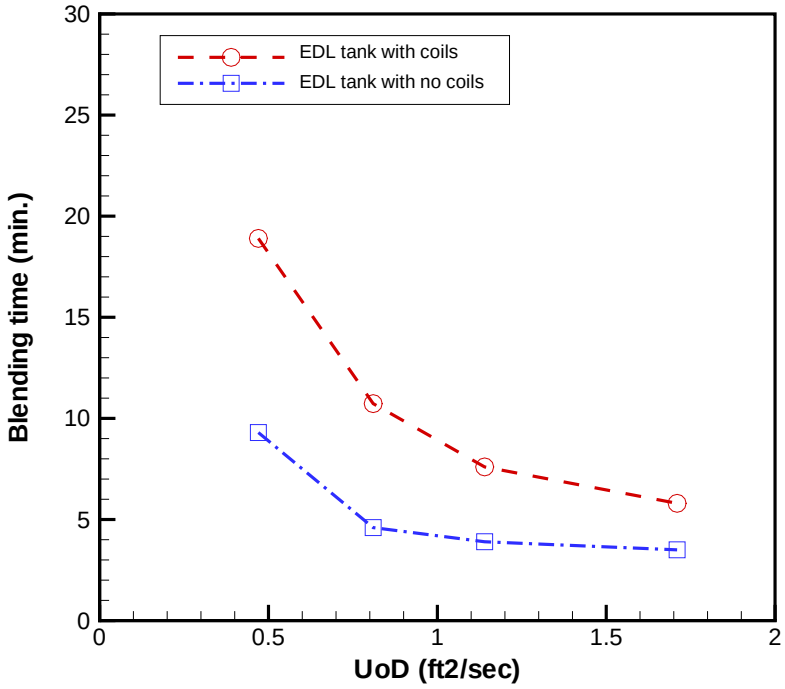

Figure 36. Impact of cooling coils on the blending time for the water-acid blending time

Table 15. Quantitative comparison of blending times for two different tank scales with T-shape and V-shape pumps

Tank scale	Coil presence inside EDL tank	Pumping fluid-tracer	$U_o d_o$ (ft^2/sec)	Blending time (min.)	
				T-shape pump	V-shape pump
EDL scale (1/10.85th)	No	Water-acid	0.47	9.3	7.6
Tank 50H	No	Water-acid	8.8	64	56

Table 16. CFD results for the cases considered for the modeling analysis

Cases	Tank scale	Cooling coils	Pump shape	Feed/Inj. fluids	$U_o d_o$ or flowrate (ft^2/sec)	Results for blending time (min.)	
						CFD	Comments
Case1	EDL scale	No	T-shape	Water/Acid	0.81	4.6	Test: 4.7
Case1	EDL scale	No	T-shape	Water/Acid	1.1	3.9	-
Case1	EDL scale	No	T-shape	Water/Acid	1.7	3.5	-
Case 2	EDL scale	No	T-shape	Nitrate/Acid	0.81	7.20	Test: 7.52
Case 3	EDL scale	Yes	T-shape	Water/Acid	0.81	10.73	Test: 12.51
Case 4	EDL scale	Yes	T-shape	Nitrate/Acid	0.81	11.03	
Case 5	EDL scale	No	T-shape	Water/Acid	0.47	9.3	
Case 6	EDL scale	Yes	T-shape	Water/Acid	0.47	18.9	
Case 7	Full scale	No	T-shape	Water/Acid	8.8	64.0	
Case 8	Full scale	Yes	T-shape	Water/Acid	8.8	99.5	
Case 9	Full scale	Yes	T-shape	Nitrate/Acid	8.8	100.7	
Case 10	EDL scale	No	V-shape	Nitrite/Acid	0.47	8.1 (0.28 ft/sec)	
Case 11a	EDL scale	No	CW/ parallel	Nitrate/Acid	0.58	7.4 (0.36 ft/sec)	
Case 11b	EDL scale	No	V-shape	Nitrite/Acid	0.58	7.5 (0.36 ft/sec)	
Case 12a	EDL scale	Yes	V-shape	Nitrate/Acid	0.70	13.5	
Case 12b	EDL scale	Yes	CW/ parallel	Nitrite/Acid	0.70	(0.45 ft/sec)	
Case 13	Full scale	No	CW/parallel	Nitrate/Acid	6.3	(0.42 ft/sec)	
Case 13a	Full scale	No	CW/parallel	Water/Acid	8.8	60 min.	(for blending time in V-shape pump)
Case 14	Full scale	Yes	CW/parallel	Nitrate/Acid	7.6	140.0	

Table 16. CFD results for the cases considered for the modeling analysis (Continued)

Cases	Tank scale	Cooling coils	Pump shape	Feed/Injection fluids	$U_o d_o$ or flowrate (ft^2/sec)	Results (min.)	
						CFD	Comments
Case15	EDL scale	No	Transfer pump with no solid plate	Nitrite	1.1 gpm	(0.142 ft/sec)	Δh = 9/16”
Case16a	EDL scale	No	Transfer pump with solid plate	Nitrite	1.1 gpm	(0.028 ft/sec)	Δh = 3/8”
Case16b	EDL scale	No	Transfer pump with solid plate	Nitrite	1.1 gpm	(0.046 ft/sec)	Δh = 1/4”
Case 17a	Full scale	No	CW/parallel	Nitrite	130 gpm	(0.021 ft/sec)	Δh = 5.43” (6” screen height)
Case 17b	Full scale	No	CW/parallel	Nitrite	130 gpm	0.016 ft/sec)	Δh = 9.5” (2” screen height)
Case 17c	Full scale	No	CW/parallel	Nitrite	130 gpm	(0.026 ft/sec)	Δh = 5.43” (4” screen height)
Case 18	Full and small scales	Yes	By 2-D approach	Water	A range of flowrates		Initial qualitative scoping study
Case 19	Full scale	Yes	CW final	Nitrate/Acid	6.1	159.2	
Case 19a	Full scale	Yes	CW final	Nitrate/Acid	6.1	(0.325 ft/sec)	Frictionless BC used at top sludge surface
Case 20	Full scale	No	CW final	Nitrate/Acid	5.1	82.7	
Case 20a	Full scale	No	CW final	Nitrate/Acid	5.1	(0.300 ft/sec)	Frictionless BC used at top sludge surface

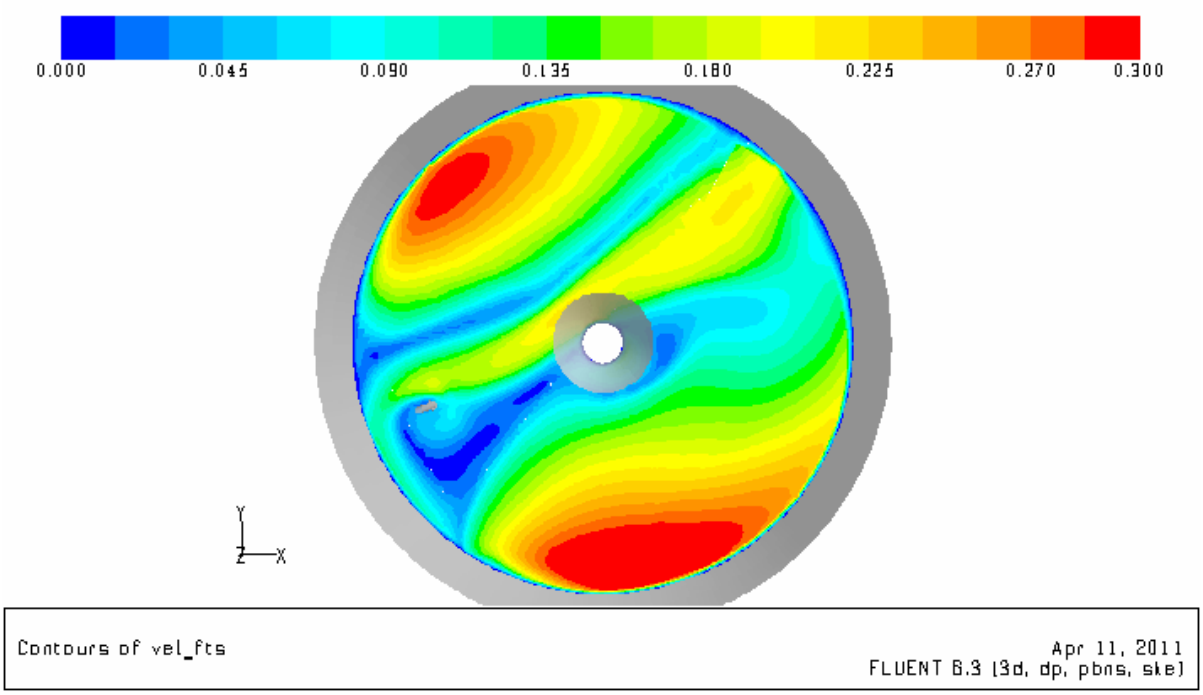

(Flow contours at top of sludge layer for the full-scale uncoiled tank with final CW pump, $U_o d_o$ = 5.1 ft^2/sec)

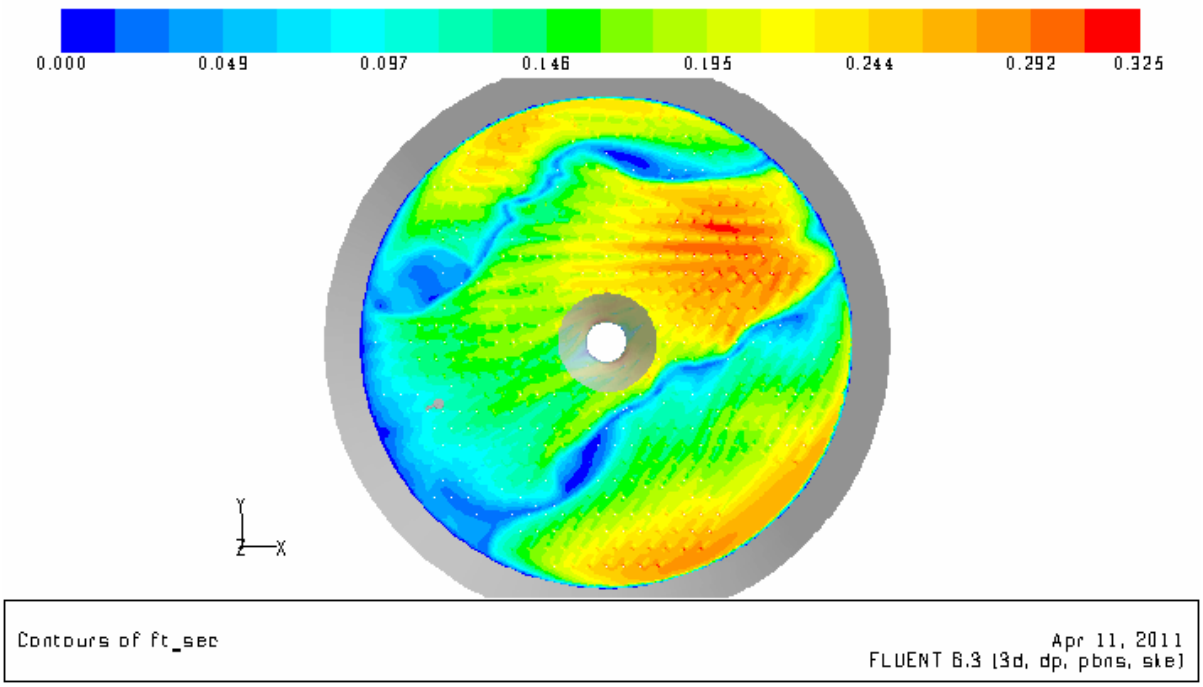

(Flow contours at top of sludge layer for the full-scale coiled tank with final CW pump, $U_o d_o$ = 6.1 ft^2/sec)

Figure 37. Comparison of flow velocity distributions for the final CW pump inside the full-scale tank with and without cooling coils

6.0 CONCLUSIONS AND SUMMARY

The transient CFD governing equations consisting of three momentum equations, one mass balance, two turbulence transport equations for kinetic energy and dissipation rate, and one species transport were solved by an iterative technique until the species concentrations of tank fluid were in equilibrium. The steady-state flow solutions for the entire tank fluid were used for flow pattern analysis for velocity scaling analysis, and the initial conditions for transient blending calculations. A series of the modeling calculations were performed to estimate the blending times for various jet flow conditions, and to investigate the impact of the cooling coils on the blending time of the tank contents. The modeling results were benchmarked against the pilot scale test results. All of the flow and mixing models were performed with the nozzles installed at the mid-elevation, and parallel to the tank wall.

From the CFD modeling results, the main conclusions are made as follows:

- The CFD flow velocity and blending modeling results are in good agreement with the SRNL scale-model test results.
- An empirical equation [Grenville and Tilton, 1997] for a tank with no cooling coils agrees with the current CFD modeling results for the dual jet.
- From the sensitivity study of the cooling coils, it was found that the tank mixing time for the coiled tank was about two times longer than that of the tank fluid with no coils under the $1/10^{th}$ scale; while the coiled tank required only 50% longer than the one without coils under the full scale Tank 50H. In addition, the time difference is reduced when the pumping $U_o d_o$ value is increased for a given scale tank.
- The blending time for T-shape, dual-jet pump is about 20% longer than that of 15^o upward V-shape pump under the $1/10^{th}$ pilot-scale tank, while the time difference between the two pumps is about 12% for the full-scale Tank 50H. These results are consistent with the literature information.
- The experimental observations done by the EDL pilot-scale test show that local fluid motions driven by the blending pump operating at 0.58 ft^2/sec pumping flow entrain negligible amount of solids from the sludge layer settled on the tank floor. Based on these experimental results, the validated CFD model computed maximum local velocity at the top sludge surface, 0.36 ft/sec. The maximum velocity was established as critical scouring criterion to prevent the sludge solids entrainment during the blending operations in a 85 ft tank. This velocity criterion was confirmed by the performance calculations for the final CW design.
- A transfer pump with a solid-plate suction screen operating at 130 gpm can be located 9.5 inches above settled sludge for 2 in screen height in a 85 ft waste tank without disturbing any sludge. Detailed results are summarized in Table 13.

Final pump performance calculations were made by using the established CW pump design, and the operating conditions to satisfy the two requirements of minimum sludge disturbance, and adequate blending of tank contents. The final calculations were performed to evaluate sludge disturbance due to blending pumps with a $U_o d_o$ value of 6.1 ft^2/sec (Case 19) for salt solutions in Tank 50H with cooling coils, and for a pump with a $U_o d_o$ value of 5.1 ft^2/sec (Case 20) for Tank 50H with no cooling coils. In addition, the blending times for the tank with and without cooling coils were estimated by the final two

models. The modeling results show that the blending times for the coiled and uncoiled tanks are 159 and 83 minutes, respectively. All the results are summarized in Table 16.

7.0 REFERENCES

1. S. Y. Lee, R. A. Dimenna, R. A. Leishear, D. B. Stefanko, "Analysis of Turbulent Mixing Jets in a Large Scale Tank", ASME *Journal of Fluids Engineering*, Volume 130, Number 1, pp. 011104, 2008.
2. S. Y. Lee and R. A. Dimenna, "Validation Analysis for the Calculation of a Turbulent Free Jet in water Using CFDS-FLOW3D and FLUENT (U)", WSRC-TR-95-0170, May 1995.
3. DWG# W706692 BLDG 241-51H Additional Waste Storage Tanks Top Slab Plan & Risers Tank 50H Steel, Rev. 24, October 18, 1993.
4. DWG# W708852 BLDG 241H Waste Storage Facility FY78 Cooling Coil Elev T48 – T51, Rev. 8, July 29, 1989.
5. ANSYS FLUENT 6.3, September 2006.
6. N. V. Chadrasekhara Swamy and P. Bandyopadhyay, "Mean and Turbulence Characteristics of Three-Dimensional Wall Jets", *Journal of Fluid Mechanics*, Vol. 71, Part 3, pp. 541-562 (1975).
7. Abramovich, G. N., "*The Theory of Turbulent Jets*", The MIT Press, Cambridge, MA, 1963.
8. S. Y. Lee, R. A. Dimenna, R. A. Leishear, and D. B. Stefanko, "Mixing in Large Scale Tanks Part I; Flow Modeling of Turbulent Mixing Jets", HT-FED2004-5622, 2004 ASME Heat Transfer / Fluids Engineering Summer Conference, Charlotte, N. C., July 11-15, 2004.
9. R. A. Dimenna, S. Y. Lee, and D. A. Tamburello, "Advanced Mixing Models", SRNL-STI-2011-00026, Svannah River National Laboratory, February 2011.
10. C. Eckart, "An Analysis of the Stirring and Mixing Processes in Incompressible Fluids", J. Mar. Research, vol. 7, pp. 265 – 275, 1948.
11. D. B. Spalding, "Mixing and Chemical Reaction in Steady Confined Turbulent Flames", 13th International Symposium on Combustion, 649-657, 1971.
12. P. L. Miller, 1991, "Mixing in High Schmidt Number Turbulent Jets", PhD Thesis, California Inst. of Technology.
13. H. B. Fischer, "Longitudinal Dispersion and Turbulent Mixing in Open-Channel Flow", Annual Review of Fluid Mechanics, Vol. 5, pp. 59-78, 1973.
14. J. Baldyga and J. R. Bourne, "A Fluid Mechanical Approach To Turbulent Mixing and Chemical Reaction, Part III Computational and Experimental Results for the New Micromixing Model", CHEM. Eng. Commun., Vol. 28, pp. 259-281, 1984.
15. J. J. Perona, T. D. Hylton, E. L. Youngblood, and R. L. Cummins, "Jet Mixing of Liquids in Long Horizontal Cylindrical Tanks", Ind. Eng. Res., Vol. 37, pp. 1478-1482, 1998.
16. R. K. Grenville and J. N. Tilton, "A New Theory Improves the Correlation of Blend Time Data from Turbulent Jet Mixed Vessels", Trans. Inst. of Chem. Eng., Vol. 74, Part A., pp. 390-396, April 1996.
17. R. K. Grenville and J. N. Tilton, "Turbulent Flow or Flow as a Predictor of Blend Time in Turbulent Jet Mixed Vessels", Proceedings of 9th European Conf. on Mixing, pp. 67-74, 1997.
18. M. Simon and C. Fonade, "Experimental Study of Mixing Performances Using Steady and Unsteady Jets", The Canadian J. of Chem. Eng., Vol. 71, 1993.

19. Forstall, W., Jr. and Shapiro, A. H., “Momentum and Mass Transfer in Coaxial Gas Jets”, *Journal of Applied Mechanics*, pp. 399-408, December 1950.
20. Ricou, F. P. and Spalding, D. B., “Measurements of Entrainment by Axisymmetrical Turbulent Jets”, *Journal of Fluid Mechanics*, Vol. 11, pp. 21-32, 1961
21. Fossett, H. and Prosser, L. E., “The Application of Free Jets to the Mixing of Fluids in Bulk”, J. of Inst. of Mechanical Engineers, Vol. 160, No. 2, pp. 224-232, 1949.
22. E. A. Fox and V. E. Gex, “Single-phase Blending of Liquids”, A.I.Ch.E. Jorunal, Vo. 2, No. 4, pp. 539-544, December 1956.
23. Okita, N. and Oyama, Y., “Mixing Characteristics in Jet Mixing”, Chemical Engineering, The Society of Chemical Engineers, Japan, Vol. 1, No. 1, pp. 92-101, 1963.
24. Lane, A. G. C. and Rice, P., “An Investigation of Liquid Jet Mixing Employing an Inclined Side Entry Jet”, Inst. of Chemical Engineers, Vol. 60, pp. 171-176, 1982.
25. W. M. Kays and M. E. Crawford, *Convective Heat and Mass Transfer*, Second Edition, McGraw-Hill Book Company, New York, 1980.
26. Kiser, K. M., “Material and Momentum Transport in Axisymmetric Turbulent Jets of Water”, *A.I.Ch.E. Journal*, Vol. 9, No. 3, pp. 386-390, 1963.
27. Post, S., 1998, “A Computational and Experimental Study of Near-Field Entrainment in Steady Gas Jets,” MSME thesis, Purdue University.
28. Hinze, J. O., *Turbulence, Second Edition*, McGraw-Hill, New York, p. 72, 1975.
29. Tennekes, H. and Lumley, J. L., *A First Course in Turbulence*, The MIT Press, Cambridge, 1972.
30. Leishear, R. A., Poirier, M. R., and Fowley, M. D., “SDI Blend and Feed Blending Pump Design Phase 1 (U)”, Savannah River National Laboratory, SRNL-STI-2010-00054, March 2010.
31. Leishear, R., Folwey, M., Poirier, M., Steeper,T., 2010,“Cooling Coil Effects On Blending in a Pilot Scale Tank”, AIChE Annual Conference, New York, New York
32. Leishear, R. A., Fowley, M. D., Poirier, M. R., Lee, S. Y., Parkinson, K. S., and Steeper, T. J., 2011, “Incipient Sludge Mixing in Nuclear Waste Tanks During Salt Blending “, Waste Management 2011 Conference, 2011, Phoenix, AZ, Paper No. 11086.